

**PHOTONS AND PHOTON STATISTICS:
FROM INCANDESCENT LIGHT TO LASERS**

RALPH v. BALTZ
*Institut für Theorie der Kondensierten Materie
Universität Karlsruhe, D-76128 Karlsruhe, Germany* *

1. Introduction

The majority of experiments in optics can be understood on the basis of Classical Electrodynamics. Maxwell's theory is perfectly adequate for understanding diffraction, interference, image formation, and even nonlinear phenomena such as frequency doubling or mixing. However, many fascinating quantum effects like correlations between photons are not captured, e.g., the photons in a single mode laser well above the threshold photons are completely uncorrelated, whereas photons in thermal light have a tendency to "arrive" in pairs.

This contribution addresses the following questions:

- What is a photon?
- Description and examples of relevant photon states.
- Discussion of basic optical devices and measurements.

2. Nature of light

2.1. HISTORICAL MILESTONES

Isaac Newton (1643 – 1727):	Founder of the corpuscular theory.
Christian Huyghens (1629 – 1695):	Founder of the wave theory of light.
Thomas Young (1773 – 1829):	Independent pioneering work about waves & interference.
Augustin Fresnel (1788 – 1827):	
James C. Maxwell (1831 – 1879):	Theory of the Electromagnetic Field.
Heinrich Hertz 1888:	Discovery of electromagnetic waves.

* <http://www-tkm.uni-karlsruhe.de> (e.g, for previous Erice contributions).

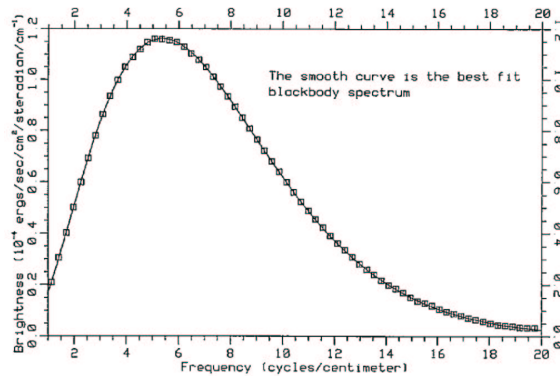


Figure 1. A perfect Planckian: The $T = 2.7\text{K}$ cosmic background radiation. From[14].

Maxwell’s theory of the Electromagnetic Field (EMF) did not only give a beautiful unification of electric and magnetic phenomena but it also predicted the existence of electromagnetic waves as undulations of electric and magnetic fields propagating through space. Wave theory had won a glorious victory! But then the incomprehensible happened:

Max Planck 1900:	Quantization of mode-oscillators.
Phillip Lenard 1902:	Difficulties with photoelectric effect.
Albert Einstein 1905:	Postulate of light quanta of energy $\hbar\omega$.
G. I. Taylor 1909:	Interference with “single photons”.
A. H. Compton 1923:	Photons have $E(\mathbf{p}) = c \mathbf{p} $.
E.O.Lawrence, J.W.Beams 1927:	No photoelectron delay time.
P. A. M. Dirac 1927	Quantum Theory of the EMF.

The era of quantum physics started with Planck’s[1] derivation of the black body spectrum in terms of quantized mode oscillators which is depicted in Fig. 1. The spectral energy density (energy per volume, energy $\hbar\omega$, polarization degree, and solid angle $d\Omega$) reads

$$e(\hbar\omega, T)d(\hbar\omega) d\Omega = \frac{(\hbar\omega)^2}{(2\pi c\hbar)^3} \frac{\hbar\omega}{e^{\frac{\hbar\omega}{k_B T}} - 1} d(\hbar\omega) d\Omega. \quad (1)$$

Lenard’s[2] observations on the photoelectric effect were incompatible with the predictions of the Maxwell–Theory where energy is distributed continuously in space. The photocurrent was found to be proportional to the intensity I of the light, however the energy of individual electrons did not depend on I , yet it increased with light frequency. Nevertheless, Lenard thought that the light does not supply the energy which is necessary to release an electron but merely triggers the photoelectric emission.

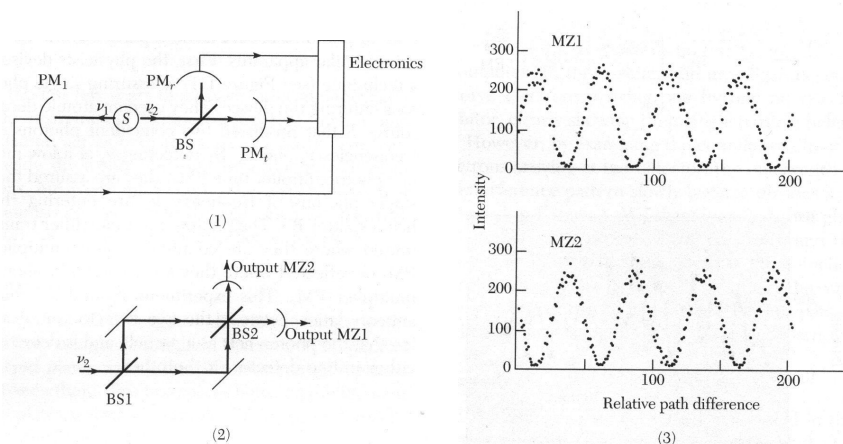


Figure 2. (1) Triggered photon cascade experiment to produce single photon states. (2) Mach-Zehnder Interferometer. (3) Number counts in the outputs of the photodetector MZ1 and MZ2 as a function of the path difference between the arms of the interferometer. (One channel corresponds to a variation of $\delta = \lambda/50$). According to Grangier et al.[11].

In 1905 Einstein published three seminal contributions: About Brownian motion, special relativity, and the photoelectric effect. For the latter contribution entitled *Über einen die Erzeugung und Verwandlung des Lichts betreffenden heuristischen Gesichtspunkt*[3] he was awarded the Nobel prize in 1921. Guided by an ingenious thermodynamic approach of the black body radiation he got the inspiration that the energy transported by light is distributed in a granular rather than in a continuous fashion in space (“darts of energy”[4]). The most direct evidence of the particle nature of light quanta is provided by the Compton-effect[5].

The existence of light quanta is in apparent contradiction with typical wave properties like interference fringes. It was expected that such fringes fade out if the intensity of the incident light becomes smaller and smaller so that the probability of having more than a single photon in the spectrometer becomes negligible. Interference experiments at very low intensity were carried out in 1909 by Taylor[6] and later, by Dempster and Batho[7], and by Janossy et al.[9]. With great disappointment all these investigators reported a null result. This discovery lead Dirac to the famous statement “a photon interferes (only) with itself”. Since 1985, coherence experiments with genuine single photon states of light are possible, see Fig. 2.

With a simple but ingenious method Lawrence and Beams[8] studied in 1927 the time variation of the photoelectric emission from a metal surface illuminated by light flashes of 10^{-8} s duration. It was found that photoelectric emission starts in less than 3×10^{-9} s after the beginning of the illumination of a potassium surface. From another experiment which was designed to

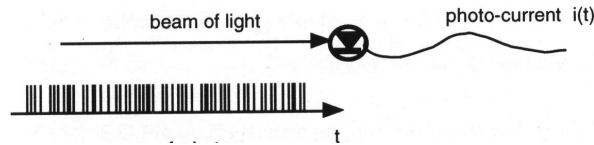


Figure 3. Photoelectric detection. The “comb” refers to a the response of a photodetector with high time resolution rather than to the incoming photons. According to Bachor[38].

investigate beats between two incoherent(!) light sources by photoelectric mixing Forrester et al.[10] deduced that $t_{del} < 10^{-10}$ s.

Further milestones are:

R. Hanbury Brown 1954	Discovery of photon bunching.
Kimble, Dagenais, Mandel 1977	Generation of nonclassical light.
R. E. Slusher, B. Yurke 1985	Generation of squeezed states

2.2. WHAT IS A PHOTON?

The photon hypothesis relies on four basic facts:

- Point-like localization of energy.
- Transport of energy and momentum through space with $E(\mathbf{p}) = c|\mathbf{p}|$.
- Absence of a delay time for the emission of photoelectrons.
- A photon interferes with itself.

Evidences for the particle nature of the excitations of the EMF are the photoelectric effect[2] and the Compton effect[5], respectively. The non-existence of a delay time[8, 10] is less frequently mentioned although it is equally important as the other properties.

Today our interpretation of photons differs substantially from the original idea of small energy “bullets” or “darts”[4]

- Photons are just the energy eigenstates of the EMF.
- The localization arises as the outcome of a measurement which causes the state of the EMF to “collapse” into an eigenstate of the device as a result of a position measurement, e.g., the absorption of a photon by an atom or in a pixel of a CCD-camera.

Although photons (in free space) have a definite energy–momentum relation, photons are not “objects” in the sense of individual, localizable classical particles. By contrast, they are indistinguishable, nonlocalizable and obey Bose statistics. A figure like Fig. 3 is dangerous as it pretends that photons in a light beam have well defined positions. The notion of classical and quantum particles is intrinsically very different. In particular

the collapse of the quantum state is foreign to all classical (wave-) theories, in particular, a localization smaller than the wavelength is not possible. The nonexistence of a waiting time for the photoelectrons is simply the consequence of statistics, some come promptly, others come later. This will be discussed in Section 5.3.

It was left to Dirac[12] to combine the wave- and particle like aspects of light so that this description is capable of explaining all interference and particle phenomena of the EMF. We shall follow his traces in Section 4.

For an excellent survey on photons see Paul's book[32]. Alternative theories are, e.g., discussed in the Rochester Proceedings from 1972[47].

3. Classical Description of the EMF: Waves

3.1. MAXWELL-EQUATIONS

For our purposes a detailed knowledge how to calculate field configurations for specific systems is not required. However, we have to know the relevant dynamical variables of the EMF.

The state of the EMF is described by two (mathematical) vector fields \mathcal{E}, \mathcal{B} which are coupled to the charge and current density of matter ρ, \mathbf{j} by the Maxwell-Equations¹

$$\frac{\partial \mathcal{E}}{\partial t} - c^2 \text{curl } \mathcal{B} = -\frac{1}{\epsilon_0} \mathbf{j}(\mathbf{r}, t), \quad \text{div } \mathcal{E} = \frac{1}{\epsilon_0} \rho(\mathbf{r}, t), \quad (2)$$

$$\frac{\partial \mathcal{B}}{\partial t} + \text{curl } \mathcal{E} = 0, \quad \text{div } \mathcal{B} = 0. \quad (3)$$

Analogous to the interpretation of Classical Mechanics one may view the two differential equations (lhs) with respect to time as equations of motion of the Maxwell field, whereas the rhs-set represents "constraints". Hence, from the 6 components of \mathcal{E}, \mathcal{B} at most 6-2=4 components are independent dynamical variables at each space point. Therefore, potentials Φ, \mathcal{A} are more appropriate than \mathcal{E}, \mathcal{B}

$$\mathcal{E} = -\dot{\mathcal{A}}(\mathbf{r}, t) - \text{grad } \Phi(\mathbf{r}, t), \quad (4)$$

$$\mathcal{B} = \text{curl } \mathcal{A}(\mathbf{r}, t). \quad (5)$$

In contrast to \mathcal{E}, \mathcal{B} the potentials \mathcal{A}, Φ are not uniquely determined, rather $\mathcal{A} \rightarrow \mathcal{A}' = \mathcal{A} + \text{grad } \Lambda(\mathbf{r}, t), \Phi \rightarrow \Phi' = \Phi - \dot{\Lambda}(\mathbf{r}, t)$ lead to the same \mathcal{E}, \mathcal{B} -fields and, hence, contain the "same physics". $\Lambda(\mathbf{r}, t)$ is an arbitrary gauge function. This property is called gauge invariance or gauge symmetry and it is considered as a fundamental principle of nature.

¹ Vectors are set in boldface, electromagnetic fields in caligraphic style.

In Quantum Optics (and in solid state physics as well), the *Coulomb gauge*, $\text{div } \mathcal{A} = 0$, is particularly convenient, as the equations for Φ and \mathcal{A} decouple

$$\Delta\Phi(\mathbf{r}, t) = -\frac{1}{\epsilon_0}\rho(\mathbf{r}, t), \quad (6)$$

$$\Delta\mathcal{A}(\mathbf{r}, t) - \frac{1}{c^2}\frac{\partial^2\mathcal{A}(\mathbf{r}, t)}{\partial t^2} = -\mu_0\mathbf{j}_{tr}(\mathbf{r}, t), \quad (7)$$

where

$$\mathbf{j}_{tr}(\mathbf{r}, t) = \mathbf{j}(\mathbf{r}, t) - \epsilon_0\text{grad}\frac{\partial\Phi(\mathbf{r}, t)}{\partial t} \quad (8)$$

denotes the so-called transverse component of the current, $\text{div } \mathbf{j}_{tr} = 0$. Some advantages of the Coulomb gauge are:

- Φ is not a dynamical system, i.e. there is no differential equation with respect to time, hence, $\Phi(\mathbf{r}, t)$ follows $\rho(\mathbf{r}, t)$ without retardation!
- As $\text{div } \mathbf{j}_{tr} = 0$ only 2 of the 3 components of \mathcal{A} are independent variables of the EMF.

3.2. MODES AND DYNAMICAL VARIABLES

In order to extract the dynamical variables of the EMF from Eq. (7) we decompose the vector potential in terms of modes $\mathbf{u}_\ell(\mathbf{r})$

$$\mathcal{A}(\mathbf{r}, t) = \sum_{\ell} A_{\ell}(t) \mathbf{u}_{\ell}(\mathbf{r}), \quad (9)$$

$$\Delta\mathbf{u}_{\ell}(\mathbf{r}) + \left(\frac{\omega_{\ell}}{c}\right)^2 \mathbf{u}_{\ell}(\mathbf{r}) = 0, \quad \text{div } \mathbf{u}_{\ell}(\mathbf{r}) = 0, \quad (10)$$

$$\int \mathbf{u}_{\ell}^*(\mathbf{r}) \mathbf{u}_{\ell'}(\mathbf{r}) d^3\mathbf{r} = \delta_{\ell, \ell'}. \quad (11)$$

In addition, there will be boundary conditions for \mathcal{E}, \mathcal{B} which fix the eigenfrequencies ω_{ℓ} of the modes labelled by ℓ . (To lighten the notation we omit the index “tr” from now on). The set of $\mathcal{A}_{\ell}(t)$ represents the generalized coordinates or dynamical variables of the EMF which obeys the equation of motion

$$\ddot{A}_{\ell}(t) + \omega_{\ell}^2 A_{\ell}(t) = \frac{1}{\epsilon_0} j_{\ell}(t). \quad (12)$$

$\mathbf{j}_{\ell}(t)$ is defined in the same way as in Eq. (9) and it can be obtained by using the orthogonality relations Eq. (11). Note, each mode is equivalent to a driven harmonic oscillator. A state of the EMF is, thus, specified by the set of mode amplitudes $A_{\ell}(t_0)$ and their velocities $\dot{A}_{\ell}(t_0)$ at a given instant of time t_0 .

$\mathcal{A}(\mathbf{r}, t)$ is a real field so that $\mathbf{u}_\ell(\mathbf{r})$ as well as $A_\ell(t)$ ought to be real. Nevertheless, the choice of complex modes may be convenient. In particular, in free space we will use “running plane waves”.

$$\mathbf{u}_{\mathbf{k},\sigma}(\mathbf{r}, t) = \frac{1}{\sqrt{V}} \boldsymbol{\epsilon}_{\mathbf{k},\sigma} e^{i\mathbf{k}\mathbf{r}}, \quad (13)$$

$$\boldsymbol{\epsilon}_{\mathbf{k},\sigma'}^* \cdot \boldsymbol{\epsilon}_{\mathbf{k},\sigma} = \delta_{\sigma,\sigma'}. \quad (14)$$

$\boldsymbol{\epsilon}_{\mathbf{k},\sigma}$ denotes the polarization vector which, by $\text{div } \mathbf{u} = i\mathbf{k} \cdot \boldsymbol{\epsilon}_{\mathbf{k},\sigma} = 0$, is orthogonal to the wave vector \mathbf{k} . (Here the notation “transversal” becomes manifest). The two independent polarization vectors will be labelled by $\sigma = 1, 2$. V denotes the normalization volume and, as usual, periodic boundary conditions implied. As a result, we obtain

$$\mathcal{A}(\mathbf{r}, t) = \sum_{\mathbf{k},\sigma} A_{\mathbf{k},\sigma}(t) \boldsymbol{\epsilon}_{\mathbf{k},\sigma} e^{i\mathbf{k}\mathbf{r}} = \sum'_{\mathbf{k},\sigma} \left(A_{\mathbf{k},\sigma}(t) \boldsymbol{\epsilon}_{\mathbf{k},\sigma} e^{i\mathbf{k}\mathbf{r}} + cc \right). \quad (15)$$

As $\mathcal{A}(\mathbf{r}, t)$ is a real field we must have $\mathcal{A}_{-\mathbf{k},\sigma} = \mathcal{A}_{\mathbf{k},\sigma}^*$, i.e. the amplitudes for \mathbf{k} and $-\mathbf{k}$ are not independent, only those amplitudes with $k_z > 0$ are independent dynamical variables. (This is the meaning of the prime in \sum' . $k_z = 0$ requires additional investigation). Fortunately, this problem can be circumvented by a redefinition of the $A_{\mathbf{k},\sigma}$ and as a result we have[39, 48]

$$\mathcal{A}(\mathbf{r}, t) = \sum_{\mathbf{k},\sigma} \sqrt{\frac{\hbar}{2\epsilon_0\omega_{\mathbf{k}}V}} \left(a_{\mathbf{k},\sigma}(t) \boldsymbol{\epsilon}_{\mathbf{k},\sigma} e^{i\mathbf{k}\mathbf{r}} + a_{\mathbf{k},\sigma}^*(t) \boldsymbol{\epsilon}_{\mathbf{k},\sigma}^* e^{-i\mathbf{k}\mathbf{r}} \right), \quad (16)$$

$$\begin{aligned} \mathcal{E}(\mathbf{r}, t) &= -\frac{\partial \mathcal{A}(\mathbf{r}, t)}{\partial t} \\ &= \sum_{\mathbf{k},\sigma} \sqrt{\frac{\hbar}{2\epsilon_0\omega_{\mathbf{k}}V}} \left(i\omega_{\mathbf{k}} a_{\mathbf{k},\sigma}(t) \boldsymbol{\epsilon}_{\mathbf{k},\sigma} e^{i\mathbf{k}\mathbf{r}} + cc \right), \end{aligned} \quad (17)$$

$$\begin{aligned} \mathcal{B}(\mathbf{r}, t) &= \text{curl } \mathcal{A}(\mathbf{r}, t) \\ &= \sum_{\mathbf{k},\sigma} \sqrt{\frac{\hbar}{2\epsilon_0\omega_{\mathbf{k}}V}} \left(i(\mathbf{k} \times \boldsymbol{\epsilon}_{\mathbf{k},\sigma}) a_{\mathbf{k},\sigma}(t) e^{i\mathbf{k}\mathbf{r}} + cc \right). \end{aligned} \quad (18)$$

In order to make the $a_{\mathbf{k},\sigma}$ dimensionless and in anticipation of the quantum treatment \hbar has been “smuggelt in”. In contrast to Eq. (12) $a_{\mathbf{k},\sigma}(t)$ obeys the first order differential equation

$$\frac{da_{\mathbf{k},\sigma}(t)}{dt} + i\omega_{\mathbf{k}} a_{\mathbf{k},\sigma}(t) = i\sqrt{\frac{1}{2\epsilon_0\hbar\omega_{\mathbf{k}}}} j_{\mathbf{k},\sigma}(t), \quad (19)$$

which has been already used performing the time-derivative of $\mathcal{A}(\mathbf{r}, t)$ in Eq. (17). (The contribution from \mathbf{j}_{tr} drops out in the final result).

From the fields we obtain the energy (Hamiltonian) of the radiation field (including the interaction with the current) and the momentum

$$\begin{aligned} H &= \int \left(\frac{\epsilon_0}{2} \mathcal{E}_{tr}^2(\mathbf{r}, t) + \frac{1}{2\mu_0} \mathcal{B}^2(\mathbf{r}, t) - \mathbf{j}_{tr}(\mathbf{r}, t) \cdot \mathcal{A}(\mathbf{r}, t) \right) d^3\mathbf{r} \\ &= \sum_{\mathbf{k}, \sigma} \hbar\omega_{\mathbf{k}} a_{\mathbf{k}, \sigma}^* a_{\mathbf{k}, \sigma} - \sqrt{\frac{\hbar}{2\epsilon_0\omega_{\mathbf{k}}}} \left(j_{\mathbf{k}, \sigma}^*(t) a_{\mathbf{k}, \sigma} + cc \right), \end{aligned} \quad (20)$$

$$P = \int \left(\frac{1}{\mu_0} \mathcal{E}_{tr}(\mathbf{r}, t) \times \mathcal{B}(\mathbf{r}, t) \right) d^3\mathbf{r} = \sum_{\mathbf{k}, \sigma} \hbar\mathbf{k} a_{\mathbf{k}, \sigma}^* a_{\mathbf{k}, \sigma}. \quad (21)$$

(In contrast to most treatments of the subject no efforts have been made to preserve the “natural sequence” of the amplitudes $a_{\mathbf{k}, \sigma}, a_{\mathbf{k}, \sigma}^*$. Potential energy/momentum contributions from the scalar potential to Eqs. (20-21) have been omitted, see Kroll’s article[48].)

The complex amplitudes $a_{\mathbf{k}, \sigma}$ represent the dynamical variables of the EMF. Its real and imaginary parts are called *quadrature amplitudes*

$$a_{\mathbf{k}, \sigma} = X_{\mathbf{k}, \sigma}^{(1)} + iX_{\mathbf{k}, \sigma}^{(2)}, \quad (22)$$

which (apart from numerical factors) are the analogues of position and momentum of a mechanical oscillator.

Example:

In free space (without current source) the complex amplitudes of a single mode with the initial condition $a(t=0) = a_0$ reads

$$a(t) = a_0 e^{-i\omega t}, \quad (23)$$

$$X_1(t) = +\Re a_0 \cos(\omega t) + \Im a_0 \sin(\omega t), \quad (24)$$

$$X_2(t) = -\Re a_0 \sin(\omega t) + \Im a_0 \cos(\omega t). \quad (25)$$

Together with Eqs. (17,18) and $\mathbf{k} = (k, 0, 0)$, $\boldsymbol{\epsilon}_{\mathbf{k}, \sigma} = (0, 1, 0)$ this field describes a linearly polarized plane wave propagating along the x -direction.

3.3. SPECIAL STATES OF THE EMF

There are two classes of states of the classical EMF:

- Deterministic states: $a_{\mathbf{k}, \sigma}(t)$ are specified for all modes at time t_0 .
- Random (stochastic) states with a probability distribution $P(\{a_{\mathbf{k}, \sigma}\}, t)$.

In radio physics these states are termed *signals* and *noise*. Prior to the advent of the laser, the only possibility to produce radiation which is correlated over some space–time domain was to filter black body radiation with respect to frequency and spatial directions.

$$a(t) = a_0 e^{-i\omega t}, \quad (26)$$

$$P(a, t) = \delta(a - a(t)). \quad (27)$$

$$P(a) = \delta(|a|^2 - |a_0|^2). \quad (28)$$

$$P(a) = \frac{1}{\pi I_{av}} e^{-|a|^2/I_{av}}, \quad (29)$$

$$I_{av} = \langle |a|^2 \rangle. \quad (30)$$

$$P(a) \propto e^{-F(a, \tau)}, \quad (31)$$

$$F(a, \tau) = \tau \frac{1}{2} |a|^2 + \frac{1}{4} |a|^4. \quad (32)$$

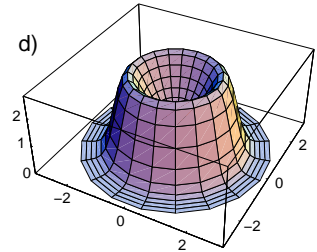
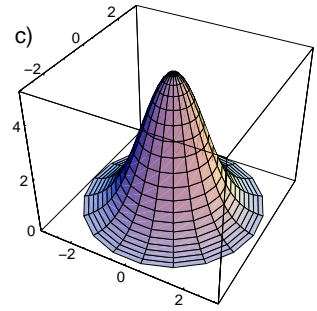
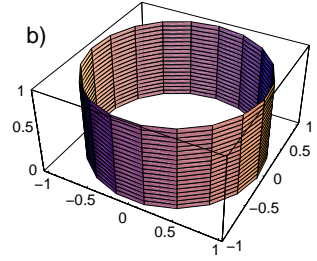
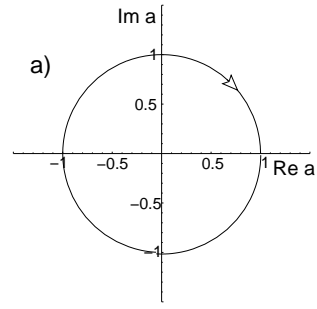


Figure 4. Model probability distributions for the complex field amplitude a of a single mode. Ideal Laser (a), amplitude stabilized laser with phase fluctuations (b), Gaussian (=thermal) noise (c). (d) Laser model which includes both amplitude and phase fluctuations according to a “phase transition” far from equilibrium. $F(a, \tau)$ is a “Ginzburg–Landau free energy” and τ is the pump parameter[33].

4. Quantum Theory of Light: Photons

4.1. CANONICAL QUANTIZATION

There are two ways to construct a quantum version of classical theory (if at all possible !). The first one is based on the Lagrangian formulation of the classical theory and it uses the Feynman path integral. We shall follow, however, the second, conventional “trail” called *canonical quantization* which is based on a Hamiltonian form, state vectors, and the Schrödinger equation. Here we have to perform the following steps:

- Classical theory in Hamiltonian form, i.e. identify (real) canonical variables p_j, q_k with Poisson-brackets $\{p_j, q_k\} = \delta_{j,k}$. (All other brackets being zero, regardless of components j, k). Rewrite all physical quantities (=observables) in terms of canonical variables.

To bring a classical theory in Hamiltonian form (if possible) one has to begin with a Lagrangian formulation. Canonical momenta are identical with “generalized momenta” defined as derivative of the Lagrangian with respect to the generalized coordinates.

- States (more precise pure states) are described by (normalized) state vectors $|\psi\rangle$ which are elements of a Hilbert space \mathcal{H} with a scalar product.

$$\langle\psi_1|\psi_2\rangle = \langle\psi_2|\psi_1\rangle^*. \quad (33)$$

- “Quantization” is obtained by the translation rule

$$\{A, B\} \rightarrow \frac{i}{\hbar} [\hat{A}, \hat{B}], \quad [\hat{A}, \hat{B}] = \hat{A}\hat{B} - \hat{B}\hat{A}. \quad (34)$$

In particular we have for canonical variables

$$[\hat{p}_j, \hat{q}_k] = -i\hbar\delta_{j,k}. \quad (35)$$

Commutators between the p 's or between the q 's themselves vanish.

- The translation rule for the operators which correspond to classical observables $G(p, q, t)$ are

$$\hat{G} = G^{cl}(p = \hat{p}, q = \hat{q}, t). \quad (36)$$

(However, there may be ambiguities with noncommuting operators. \hat{G} has to be hermitian.)

- Values of observables are defined as expectation values of the corresponding operators:

$$\langle G \rangle = \langle\psi|\hat{G}|\psi\rangle = \langle\psi|\psi'\rangle, \quad (37)$$

where $|\psi'\rangle = \hat{G}|\psi\rangle$.

- Dynamics: Initially, the system is supposed to be in state $|\psi_0\rangle = |\psi(t_0)\rangle$. Then, sequence of states $|\psi(t)\rangle$ which the system runs through as a function of time is governed by the *Schrödinger equation*

$$i\hbar \frac{\partial |\psi(t)\rangle}{\partial t} = \hat{H} |\psi(t)\rangle, \quad (38)$$

where \hat{H} denotes the *Hamiltonian* (=energy) of the system. Note, Eq. (38) holds not only for non-relativistic particles but also for photons!

- States vectors $|\psi\rangle$ describe *pure states* with zero entropy. They are the analoga of the ideal mechanical states with fixed q, p or the ideal states of the classical EMF with fixed $a_{\mathbf{k},\sigma}$ (“signals”). The counterparts of the classical statistical states, e.g., thermal radiation Eq (29), are called *mixed states*. They have nonzero entropy and are described by a *density operator* $\hat{\rho}$

$$\langle G \rangle = \text{trace} (\hat{\rho} \hat{G}). \quad (39)$$

4.2. QUANTUM OPTICS

The quantum version of the EMF together with a (nonrelativistic) theory of matter is called *Quantum Optics*. To follow the scheme outlined in the previous section we have to bring the Maxwell–Theory into a Hamiltonian form. This is, however, almost trivial because the EMF is dynamically equivalent to a system of uncoupled harmonic oscillators with generalized “coordinates” A_ℓ , see Eq. (12). We guess the Lagrangian

$$L \propto \sum_{\ell} \frac{1}{2} \dot{A}_{\ell}^2 - \frac{\omega_{\ell}^2}{2} A_{\ell}^2 + \frac{1}{\epsilon_0} j_{\ell}(t) A_{\ell} \quad (40)$$

$$= \int \left(\frac{\epsilon_0}{2} \mathcal{E}_{tr}^2(\mathbf{r}, t) - \frac{1}{2\mu_0} \mathcal{B}^2(\mathbf{r}, t) + \mathbf{j}_{tr}(\mathbf{r}, t) \cdot \mathcal{A}(\mathbf{r}, t) \right) d^3\mathbf{r}. \quad (41)$$

The canonical variables are $Q_{\ell} = A_{\ell}, P_{\ell} = \dot{A}_{\ell}$ and the Hamiltonian is obtained from $H = P\dot{Q} - L$.

For complex modes, as used in Eqs. (16–18), each amplitude contains two real variables X_1, X_2 which (apart from numerical factors) correspond to canonical momentum and position, ($p = \sqrt{2m\hbar\omega}X_2, x = \sqrt{2\hbar/m\omega}X_1, \{p, x\} = 1$). The complex amplitudes obey the Poisson bracket relations

$$\{a_{\mathbf{k},\sigma}, a_{\mathbf{k}',\sigma'}^*\} = \frac{i}{\hbar} \delta_{\mathbf{k},\mathbf{k}'} \delta_{\sigma,\sigma'}. \quad (42)$$

Quantization is obtained by replacing the classical amplitudes $a_{\mathbf{k},\sigma}, a_{\mathbf{k},\sigma}^*$ by “ladder operators” $\hat{a}_{\mathbf{k},\sigma}, \hat{a}_{\mathbf{k},\sigma}^\dagger$ with commutation relations

$$[\hat{a}_{\mathbf{k},\sigma}, \hat{a}_{\mathbf{k}',\sigma'}^\dagger] = \delta_{\mathbf{k},\mathbf{k}'} \delta_{\sigma,\sigma'}. \quad (43)$$

Field operators, Hamiltonian, and the momentum operator are (in the Schrödinger picture)

$$\hat{\mathcal{A}}(\mathbf{r}) = \sum_{\mathbf{k},\sigma} \sqrt{\frac{\hbar}{2\epsilon_0\omega_{\mathbf{k}}V}} \left(\hat{a}_{\mathbf{k},\sigma} \boldsymbol{\epsilon}_{\mathbf{k},\sigma} e^{i\mathbf{k}\mathbf{r}} + \hat{a}_{\mathbf{k},\sigma}^\dagger \boldsymbol{\epsilon}_{\mathbf{k},\sigma}^* e^{-i\mathbf{k}\mathbf{r}} \right), \quad (44)$$

$$\hat{\mathcal{E}}(\mathbf{r}) = \sum_{\mathbf{k},\sigma} \sqrt{\frac{\hbar}{2\epsilon_0\omega_{\mathbf{k}}V}} \left(i\omega_{\mathbf{k}} \hat{a}_{\mathbf{k},\sigma} \boldsymbol{\epsilon}_{\mathbf{k},\sigma} e^{i\mathbf{k}\mathbf{r}} + cc \right), \quad (45)$$

$$\hat{\mathcal{B}}(\mathbf{r}) = \sum_{\mathbf{k},\sigma} \sqrt{\frac{\hbar}{2\epsilon_0\omega_{\mathbf{k}}V}} \left(i(\mathbf{k} \times \boldsymbol{\epsilon}_{\mathbf{k},\sigma}) \hat{a}_{\mathbf{k},\sigma} e^{i\mathbf{k}\mathbf{r}} + cc \right). \quad (46)$$

$$\hat{H} = \sum_{\mathbf{k},\sigma} \hbar\omega_{\mathbf{k}} \hat{a}_{\mathbf{k},\sigma}^\dagger \hat{a}_{\mathbf{k},\sigma} - \sqrt{\frac{\hbar}{2\epsilon_0\omega_{\mathbf{k}}}} \left(j_{\mathbf{k},\sigma}^*(t) \hat{a}_{\mathbf{k},\sigma} + hc \right), \quad (47)$$

$$\hat{P} = \sum_{\mathbf{k},\sigma} \hbar\mathbf{k} \hat{a}_{\mathbf{k},\sigma}^\dagger \hat{a}_{\mathbf{k},\sigma}, \quad (48)$$

The (infinite) zero point energy which arises from the noncommutativity of the $\hat{a}_{\mathbf{k},\sigma}, \hat{a}_{\mathbf{k},\sigma}^\dagger$ operators has been omitted in the Hamiltonian as this has no influence on the dynamics of the EMF. The zero point fluctuations of the EMF, however, are still present in the fields, as we shall see later.

As it is well known, the stationary states of a (free) harmonic oscillator, $|n\rangle$, $n = 0, 1, 2, \dots$, are the eigenstates of the number operator $\hat{N} = \hat{a}^\dagger \hat{a}$. In addition, they are nondegenerate, orthogonal, and normalizable, $\langle m|n\rangle = \delta_{m,n}$. The action of the \hat{a}, \hat{a}^\dagger -operators on these states is

$$\hat{a}^\dagger \hat{a} |n\rangle = n |n\rangle, \quad (49)$$

$$\hat{a} |n\rangle = \sqrt{n} |n-1\rangle, \quad (50)$$

$$\hat{a}^\dagger |n\rangle = \sqrt{n+1} |n+1\rangle. \quad (51)$$

These operators are also called “ladder operators” because repeated operation on a particular energy eigenstate creates the “ladder” of all other states, with \hat{a}^\dagger we climb up, whereas with \hat{a} we climb down the ladder.

The states of the infinite set of mode oscillators of the EMF is, thus, labelled by the (infinite set of) quantum numbers $\{n_{\mathbf{k},\sigma}\}$ which individually can take on different nonnegative integers. These states describe the stationary states of the free EMF $|\{n_{\mathbf{k},\sigma}\}\rangle$ and their time dependence is,

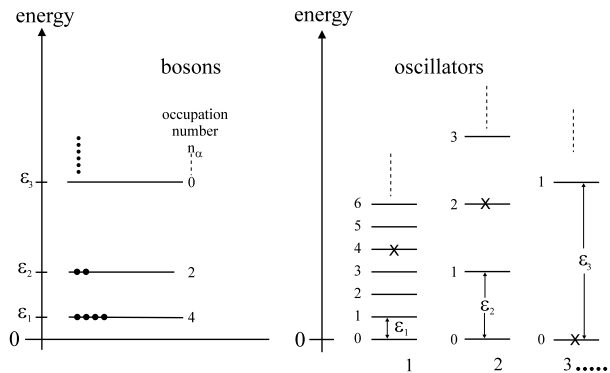


Figure 5. Equivalence of a system of N (noninteracting) bosons with single-particle energies ϵ_ℓ and occupation numbers n_ℓ and an infinite (uncoupled) set of harmonic oscillators with frequencies $\omega_\ell = \epsilon_\ell/\hbar$. Note that the zero-point energies of the oscillators are omitted. Dots symbolize particles, crosses excited states, respectively. $N = 6$. According to Ref.[49]

as usual, obtained by an exponential factor $\exp(-m\omega t)$ for each mode. All other states can be represented as a superposition of these *number states*, which, therefore, represent a natural basis for the description of the quantum states of the EMF.

For a wide-range introduction see Scully and Zubairy's book on *Quantum Optics*[35].

4.3. OSCILLATORS AND PHOTONS

Dirac[12] has made the important observation that

... a system of noninteracting bosons with single particle energies ϵ_ℓ is dynamically equivalent to a system of uncoupled oscillators and vice versa. The two systems are just the same looked at from two different points of view.

Here, *dynamic equivalence* implies that all states of an N -boson system which are conventionally described by a symmetric wave function are equally well described in the "oscillator picture", where each single particle state with energy ϵ_ℓ corresponds to an oscillator with frequency $\omega_\ell = \epsilon_\ell/\hbar$. Remarkably, the commutation relations $[\hat{a}_\ell, \hat{a}_{\ell'}^\dagger] = \delta_{\ell, \ell'}$ between the ladder operators are fully equivalent to the permutation symmetry of the boson wavefunction, and, fortunately, a great deal of notational redundancy in the description of a many-body system is removed. In addition, all operators in the particle picture (lhs of Fig. 5) can be translated into operators acting on the oscillator states. These operators are conveniently expressed in terms

of ladder operators and contain products with an equal number of $\hat{a}_{\mathbf{k},\sigma}$ and $\hat{a}_{\mathbf{k}',\sigma'}^\dagger$ operators.

The union of all sets of $N = 1, 2, \dots$ particle subspaces plus the $N = 0$ “no particle” vacuum state is called *Fock space*. The number states $|\{n_\ell\}\rangle$ are the eigenstates of the particle number operator

$$\hat{N} = \sum_{\ell} \hat{a}_{\ell}^\dagger \hat{a}_{\ell}. \quad (52)$$

Now, the particle number itself becomes a dynamical variable and we can even describe states which are not particle number eigenstates of the system. \hat{a}_{ℓ}^\dagger , \hat{a}_{ℓ} are called particle *creation and destruction operators* because they change the number of particles by one. The Fock representation is also called *occupation number representation* or “second quantization”. It is much more flexible than the original formulation with a fixed particle number.

The bosons corresponding to the quantized oscillators with $\ell = (\mathbf{k}, \sigma)$ are called *photons*. Photons behave very different from massive particles like electrons. They can be created and annihilated arbitrarily and they are not localizable. This will become obvious by the discussion of various examples in the next sections.

Example:

The momentum operator (in one dimension) is translated according to

$$\sum_{j=1}^N \hat{p}_j \rightarrow \sum_{\ell, \ell'} \langle \ell' | \hat{p} | \ell \rangle \hat{a}_{\ell'}^\dagger \hat{a}_{\ell}. \quad (53)$$

ℓ labels any set of single particle states. Evaluate the expectation value of a single particle operator for both the wave-function and occupation number representation for $N = 3$ particles! (The full advantage of the occupation number representation will really show up if interaction of particles are included.)

4.4. SPECIAL PHOTON STATES

In the following we shall discuss some selected states of the EMF with respect to the expectation values of the fields, energy, and momentum. The physically relevant states cannot be eigenstates of the electrical field operator $\hat{\mathcal{E}}$ as these have infinite energy. ($\hat{\mathcal{E}}$ corresponds to the position (or momentum) of a mechanical oscillator).

The “quantum unit” of the electrical field is $\mathcal{E}_0 = \sqrt{\hbar\omega/2\epsilon_0 V}$. For green light, $\lambda = 500\text{nm}$, and a quantization volume of $V = 1\text{cm}^3$, $\mathcal{E}_0 \approx 0.075\text{V/m}$, whereas, in a microresonator of linear dimension $1\mu\text{m}$, $\mathcal{E}_0 \approx 7.5 \times 10^4\text{V/m}$!

4.4.1. n -photons in a single mode

We consider n photons in a single mode with $\mathbf{k} = (k, 0, 0)$ and linear polarization along y -direction $\boldsymbol{\epsilon}_{\mathbf{k},\sigma} = (0, 1, 0)$. $|n\rangle$ is, of course, an eigenstate of the photon number operator Eq. (52). (Mode indices \mathbf{k}, σ are omitted, for brevity).

Without a driving current source this state is an eigenstate of the Hamiltonian with energy $\hbar\omega n$ and it evolves in time according to

$$|n, t\rangle = |n\rangle e^{-i\omega n t}. \quad (54)$$

In addition, this state is also a momentum eigenstate with eigenvalue $n\hbar\mathbf{k}$, Eq. (48). However, $|n\rangle$ is not an eigenstate of the electrical field operator, Eq. (45), because $\hat{a}_{\mathbf{k},\sigma}, \hat{a}_{\mathbf{k},\sigma}^\dagger$ changes the number of photons by ± 1 . The expectation value of the electrical field operator reads

$$\langle n, t | \hat{\mathcal{E}}(\mathbf{r}) | n, t \rangle = 0, \quad (55)$$

$$\langle n, t | \hat{\mathcal{E}}^2(\mathbf{r}) | n, t \rangle = \mathcal{E}_0^2 (2n + 1). \quad (56)$$

Certainly, such a state does not correspond to a classical sinusoidal wave, instead it is pure “quantum noise”. Note, even in the vacuum state, $|0\rangle$, *zero point fluctuations* are present.

4.4.2. Single photon wave packet

We consider a superposition of single photon states referring to different modes (but with the same polarization).

$$|\phi_\sigma(\mathbf{k}), t\rangle = \sum_{\mathbf{k}} \phi_\sigma(\mathbf{k}) e^{-i\omega_{\mathbf{k}} t} |1_{\mathbf{k},\sigma}\rangle, \quad (57)$$

where $\phi_\sigma(\mathbf{k})$ is an arbitrary normalizable function which, with some care, may be interpreted as a wave function of a photon (-wave packet) in momentum space. However, there is no reasonable photon position representation[40]. The question of localization of photons is discussed, e.g., by Clauser[50].

A special case is the superposition of just two modes. Such a “two colour state” can be created by a simultaneous excitation of two almost degenerate (atomic) states by a short laser pulse. If the bandwidth of the laser pulse embraces both components a coherent superposition of the two atomic states is created, which decays spontaneously in a single photon “wave packet” state. Experimentally, this phenomenon shows up in the form of “quantum beats”, see Fig. 6.

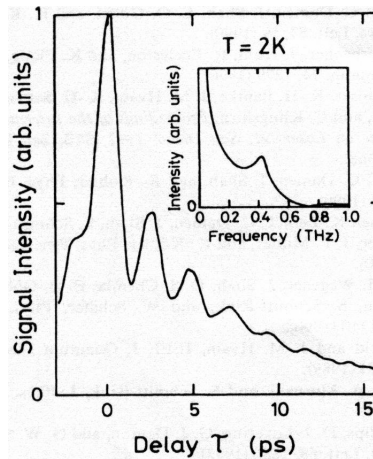


Figure 6. Quantum beats between a coherently prepared population of excitons and biexcitons in AlGaAs quantum well. According to Pandtke et al.[43].

4.4.3. Coherent states (ideal single mode laser)

We are searching for a state, in which the fields vary sinusoidally in space and time with \mathcal{E} -uncertainty as small as possible, i.e., have time independent uncertainties in the quadrature amplitudes with $\Delta X_1 = \Delta X_2 = 1/2$ and $\Delta X_1 \Delta X_2 = 1/4$. These states were already known by Schrödinger[13] and they correspond to a displaced Gaussian ground state wavefunction whose time evolution is depicted in Fig 7. In dimensionless quantities, we have

$$\psi(x, t) = (\pi)^{-1/4} \exp \left[-\frac{(x - x_c(t))^2}{2} \right] e^{i p_c(t)} e^{i \varphi(t)}. \quad (58)$$

$x_c(t)$ and $p_c(t)$ are the solutions of the classical equations of motion of the oscillator and $\varphi(t)$ is a time dependent phase.

In number representation, these states are given by (without the $\varphi(t)$ -term)

$$|\alpha\rangle = e^{-\frac{1}{2}|\alpha|^2} \sum_{n=0}^{\infty} \frac{\alpha^n}{\sqrt{n!}} |n\rangle, \quad \alpha = x_c + i p_c. \quad (59)$$

Nowadays, these states are called *coherent states*, *Glauber states*, or just α -states. Glauber[15] was the first who recognized their fundamental role for the description of laser radiation and coherence phenomena.

The α -states have a number of interesting properties:

- $|\alpha\rangle$ is an eigenstate of the destruction operator

$$\hat{a}|\alpha\rangle = \alpha|\alpha\rangle, \quad (60)$$

where α is an arbitrary complex number.

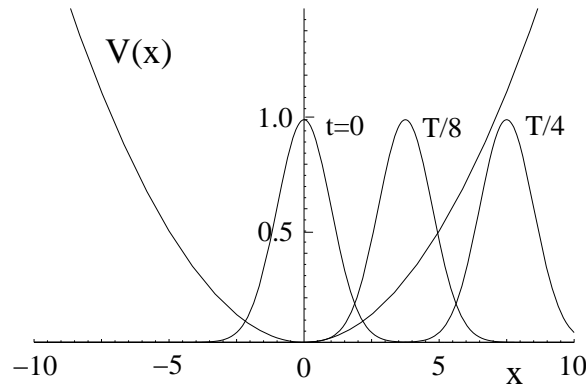


Figure 7. Time development of the coherent state wave function.

- α -states can be generated by the unitary “displacement” operator \hat{D}

$$|\alpha\rangle = \hat{D}(\alpha)|0\rangle, \quad (61)$$

$$\hat{D}(\alpha) = e^{\alpha\hat{a}^\dagger - \alpha^*\hat{a}} = e^{-\frac{1}{2}|\alpha|^2} e^{\alpha\hat{a}^\dagger} e^{-\alpha\hat{a}}, \quad (62)$$

$$\hat{D}^\dagger \hat{a} \hat{D} = \hat{a} + \alpha. \quad (63)$$

- The time dependence (even with a classical external current source) is obtained just by replacing $\alpha \rightarrow \alpha(t)$, where

$$|\alpha, t\rangle = e^{i\varphi(t)} |\alpha(t)\rangle, \quad (64)$$

Real and imaginary parts of $\alpha(t) = x_c(t) + ip_c(t)$ correspond to the position and momentum of a classical oscillator. For a free oscillator $\alpha(t) = \alpha e^{-i\omega t}$. (Phase $\varphi(t)$ has no influence on the “physics”).

- Although the α -eigenvalues form a continuous spectrum, the $|\alpha\rangle$ states are normalizable but they are not orthogonal. Moreover, the set of $|\alpha\rangle$ states is complete (overcomplete) and forms a convenient basis for an “almost classical description” of laser physics.

For further properties see e.g., Scully and Zubairy[35] or Louissell[36].

Expectation values and uncertainties of the electrical field and photon number and the probability to measure n photons are (omitting the polarization index)

$$\mathcal{E}(\mathbf{r}, t) = \langle \alpha(t) | \hat{\mathcal{E}}(\mathbf{r}) | \alpha(t) \rangle = -2\mathcal{E}_0 |\alpha| \sin(\mathbf{k}\mathbf{r} - \omega\mathbf{k}t + \phi), \quad (65)$$

$$(\Delta\mathcal{E})^2 = \mathcal{E}_0^2, \quad (66)$$

$$\langle \hat{N} \rangle = |\alpha|^2 = \bar{n}, \quad (\Delta\hat{N})^2 = \langle \hat{N} \rangle, \quad (67)$$

$$p_n = |\langle n | \alpha \rangle|^2 = e^{-\bar{n}} \frac{\bar{n}^n}{n!}. \quad (68)$$

$\alpha = |\alpha| \exp(i\phi)$. Note, the relative amount of fluctuations in the electrical field decreases with increasing amplitude, see Fig. 9. p_n denotes a *Poissonian distribution* with mean photon number $\bar{n} = |\alpha|^2$ and uncertainty $(\Delta n)^2 = \bar{n}$. Thus, in a coherent state photons behave like they were uncorrelated classical objects! In contrast to naive expectations, the photons in a (single mode) laser (and well above the threshold) “arrive” in a random fashion, in particular they do not “ride” on the electrical field maxima.

How to generate α -states? As α -states are eigenstates of the (nonhermitian) destruction operator \hat{a} , there is no corresponding observable and “measuring apparatus”! However, α -states can be simply generated from a classical current source

$$\hat{H} = \hbar\omega\hat{a}^\dagger\hat{a} - [f(t)\hat{a}^\dagger + f^*(t)\hat{a}], \quad (69)$$

where $f(t) \propto j(t)$. Nevertheless, it was a great surprise that the light-matter interaction in a laser (well above the threshold) could be modelled in such a simple way.

The amplitude of the electrical field of a laser may be well stabilized by saturation effects, but there is no possibility to control the phase, i.e., a more realistic laser state would be described by the density operator

$$\hat{\rho} = \int \frac{d\phi}{2\pi} |\alpha\rangle\langle\alpha| = \sum_n p_n |n\rangle\langle n|. \quad (70)$$

This state is made up of an (incoherent) superposition of n -photon states with a *Poissonian distribution*. A model of laser light with a finite linewidth which is caused by phase diffusion has been given by Jacobs[16].

Problem:

P1: Verify that Eqs. (58,64) are solutions of the time-dependent Schrödinger equation of the (driven) harmonic oscillator.

4.4.4. Squeezed states

Squeezed states correspond to wave functions which have an uncertainty in one of the quadrature amplitudes smaller than for the groundstate. A harmonic oscillator has the peculiarity that any wave function will reproduce itself after the classical oscillation time $T = 2\pi/\omega$, moreover, there is an exact mirror image at $t = T/2$, see Fig. 8. In particular, we will study Gaussian wave packets which initially are minimum uncertainty wave packets with $\Delta X_1 \Delta X_2 = 1/4$, but $\Delta X_1 < 1/2$, $\Delta X_2 > 1/2$ (or vice versa).

$$\Psi(x, t) = \exp\left(-\frac{x^2}{2} w(t) + xv(t) + u(t)\right). \quad (71)$$

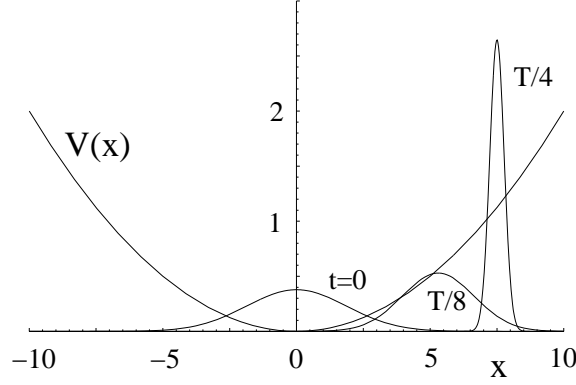


Figure 8. Time development of a squeezed state wave function.

$u(t)$, $v(t)$, and $w(t)$ can be complex. These parameters follow from an insertion in the time dependent Schrödinger equation. We leave that as an exercise.

Squeezed states are characterized by two complex variables, usually termed α and ξ and they can be constructed by first operating with the unitary squeezing operator $\hat{S}(\xi)$ on the vacuum and then by shifting with $\hat{D}(\alpha)$.

$$|\alpha, \xi\rangle = \hat{D}(\alpha) \hat{S}(\xi) |0\rangle, \quad (72)$$

$$\hat{S}(\xi) = e^{\frac{1}{2}(\xi^* \hat{a}^2 - \xi (\hat{a}^\dagger)^2)}, \quad (73)$$

$$\hat{S}^\dagger(\xi) \hat{a} \hat{S}(\xi) = \cosh(r) \hat{a} - e^{-2i\theta} \sinh(r) \hat{a}^\dagger, \quad (74)$$

where $\xi = r \exp(i\theta)$. (Some authors prefer a reversed sequence of $\hat{D}(\alpha)$ and $\hat{S}(\xi)$). Squeezed states are also the eigenstates of a transformed destruction operator \hat{b} [18]

$$\hat{b} = \mu \hat{a} + \nu \hat{a}^\dagger, \quad \mu = \cosh(r), \quad \nu = e^{-2i\theta} \sinh(r), \quad (75)$$

$$\hat{b}|\beta\rangle = \beta|\beta\rangle, \quad (76)$$

$$\beta = \alpha \cosh(r) + \alpha^* e^{-2i\theta} \sinh(r), \quad (77)$$

$$\langle \hat{N} \rangle = |\alpha|^2 + \sinh^2(r), \quad (78)$$

$$(\Delta N)^2 = |\alpha \cosh(r) - \alpha^* e^{i\theta} \sinh(r)|^2 + \frac{1}{2} \sinh^2(2r). \quad (79)$$

For moderate squeezing the photon distribution function is similar to a Poissonian, but with a narrower width, see e.g., Bachor[38] (p. 234).

Squeezed states can be generated by various nonlinear processes, e.g. degenerate parametric amplification of an initial coherent (=laser) state.

$$\hat{H}_{par} = \hbar\omega \hat{a}^\dagger \hat{a} - k \left[e^{i(\omega t + \phi_p)} \hat{a}^2 + hc \right]. \quad (80)$$

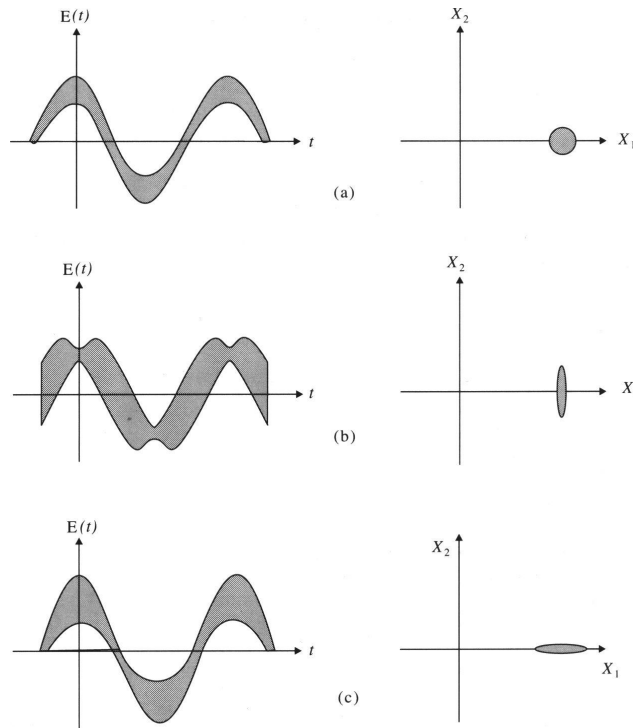


Figure 9. Contours and time dependence of the electrical field for (a) a coherent state), squeezed state with reduced quantum noise in X_1 , and (c) a squeezed state with reduced noise in X_2 . According to Caves[19].

In this model, the pump at $\omega_p = 2\omega$ is treated as a classical source; the coupling constant k is proportional to the second order susceptibility χ_2 of the nonlinear crystal. An initial α -state evolves with $\alpha(t) = \alpha \exp(-i\omega t)$ and $\xi(t) = g \exp[-i(\omega t + \phi_p - \pi/2)]$. Note, squeezing is sensitive on the phase of the pump.

A nice review of squeezed states with applications has been given by Walls[21], for details see the articles by Stoler[17], Yuen[18], and Caves[19]. Communication by squeezed light has been discussed by Giacobino et al.[22].

Problems:

P2: Calculate the functions $w(t), v(t), u(t)$ in Eq. (71).

P3: Show that \hat{b}, \hat{b}^\dagger are Bose operators, i.e., $[\hat{b}, \hat{b}^\dagger] = 1$.

P4: Which property must the energy spectrum of a system have that its state reproduces after a finite time? (See also Chergui's contribution in this book and Ref.[44]).

P5: Are there photons in a static magnetic field? (Groundstate of Eq. (47)).

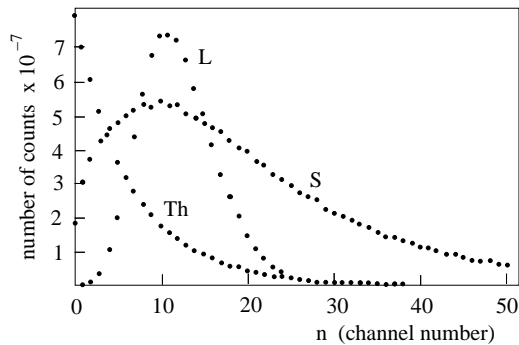


Figure 10. Photon count distribution for a single mode laser (L), thermal light (G), and a superposition of both (S). According to Arecchi[51].

4.4.5. Thermal (chaotic) photon states

A single mode of thermal (black body) radiation is described by a statistical operator

$$\hat{\rho} = \frac{1}{Z} e^{-\beta \hat{H}} = \sum_{n=0}^{\infty} b_n |n\rangle \langle n|, \quad (81)$$

$$b_n = \frac{\bar{n}^n}{(\bar{n} + 1)^{n+1}} = \frac{1}{1 + \bar{n}} \left(1 + \frac{1}{\bar{n}}\right)^{-n}, \quad (82)$$

$$\langle \hat{N} \rangle = \text{tr}(\hat{\rho} \hat{N}) = \frac{1}{e^{\beta \hbar \omega} - 1} = \bar{n}, \quad (83)$$

$$(\Delta \hat{N})^2 = \bar{n}(\bar{n} + 1). \quad (84)$$

$\beta = 1/(k_B T)$, $Z = 1/(1 - \exp(-\beta \hbar \omega))$ is the partition function, b_n the Bose-Einstein photon distribution (geometric sequence), and \bar{n} is the mean photon number in the mode. In contrast to a coherent state $\Delta \hat{N}/\bar{n} \rightarrow 1$ for $\bar{n} \rightarrow \infty$, see Fig. 10.

5. Optical devices and measurements

5.1. PHOTODETECTORS

In a classical description the electrical current of a photoelectric device like a photocell, a photomultiplier, or a photodiode is proportional to the light intensity (energy density) averaged over a cycle of oscillation

$$J_{PD} = \zeta I(t), \quad (85)$$

$$I(t) = \langle \mathcal{E}(t)^2 \rangle_{cycl} = \mathcal{E}^{(-)}(t) \mathcal{E}^{(+)}(t). \quad (86)$$

(A factor 1/2 has been included in the definition of $\langle \dots \rangle_{cycl}$). $\mathcal{E}^{(\pm)}$ denote the positive(negative) frequency parts of the electric field (polarization

properties and space variables omitted for simplicity)

$$\mathcal{E}(t) = \int_0^\infty \left(\mathcal{E}^{(+)}(\omega) e^{-i\omega t} + \mathcal{E}^{(-)}(\omega) e^{+i\omega t} \right) \frac{d\omega}{2\pi}. \quad (87)$$

For a free field $\mathcal{E}^{(\pm)}$ are identical with the first(second) terms of Eq. (17). (Note also the sign convention.) For a stochastic field, the product $\mathcal{E}^{(-)}\mathcal{E}^{(+)}$ has to be additionally averaged on the different realizations of the ensemble. In praxis ζ includes the (quantum) efficiency of the photodetector, too.

In a quantum treatment, the response of the detector arises from the ground state of the atoms in the photocathode to highly excited quasi-free states by absorption of photons. Initially, we have for the combined system “atom plus EMF” $|i\rangle = |a, \{n\}\rangle$. The electrical dipole interaction $\hat{H}_{dip} = -e\hat{\mathbf{E}}\mathbf{r}$ induces transitions to final states $|f\rangle = |b, \{n'\}\rangle$. With the golden rule and summing over all possible final states, we have for the total transition rate

$$p(t) = \zeta \langle \hat{\mathcal{E}}^{(-)}(\mathbf{r}, t) \hat{\mathcal{E}}^{(+)}(\mathbf{r}, t) \rangle, \quad (88)$$

where $\hat{\mathcal{E}}^{(\pm)}$ denote the creation/destruction parts of the electrical field operator (in the Heisenberg picture) and ζ includes the atomic dipole transition matrix element. Implicitly, we shall assume a perfect photocathode with unit quantum efficiency so that each absorbed photon causes an atom in the phototube to emit an electron and register a single count during times $t, t + dt$.

A good presentation of the quantum theory of a photodetector has been given by Glauber in the Proceedings of the Les Houches[45] and Fermi summerschools[46].

5.2. INTERFEROMETERS

Interferometers are devices to measure the correlation of the EMF between different space–time points. The prototype is the *Young double slit interference experiment* which is depicted in Fig. 11. Thermal light from a point source is rendered parallel by a lens, passes through a wavelength filter, and then falls on a screen which contains two slits or pinholes (as we assume for simplicity). Interference fringes show up on a second screen placed on the right of the first screen, many wavelengths apart. In the following discussion we shall ignore complications arising from the finite source diameter and consequent lack of perfect parallelism in the illuminating beam, diffraction effects at the pinholes (or slits), etc., in order that attention be focused on the properties of the incident EMF rather than on details of the measuring device.

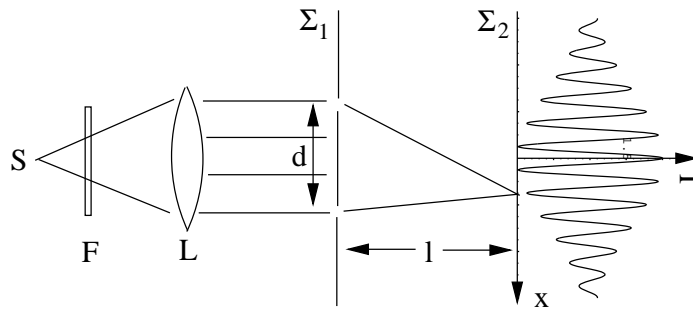


Figure 11. Arrangement of components for an idealized Young's interference experiment. Interferogram shown in the limit of infinitely small slits and $\lambda \ll d \ll L$. Gaussian spectral filter F .

Let $\mathcal{E}(\mathbf{r}, t)$ be the electrical field of the radiation at point \mathbf{r} on the observation screen at time t . This field is a superposition of the incident field at points $\mathbf{r}_1, \mathbf{r}_2$ at earlier times t_1, t_2 ,

$$\mathcal{E}(\mathbf{r}, t) = u_1 \mathcal{E}^{in}(\mathbf{r}_1, t_1) + u_2 \mathcal{E}^{in}(\mathbf{r}_2, t_2), \quad (89)$$

$$t_1 = t - s_1/c, \quad t_2 = t - s_2/c. \quad (90)$$

Coefficients u_1, u_2 depend on the geometry and they are purely imaginary since the secondary waves radiated by the pinholes (or slits) are $\pi/2$ out of phase with the primary beam. For simplicity, we consider identical pinholes and approximate $u_1 = u_2 = u_0 = \text{const}$.

The (cycle averaged) intensity of light at position \mathbf{r} can be expressed in terms of the (first order) correlation function $G_1(\mathbf{r}_2, t_2; \mathbf{r}_1, t_1)$

$$I(t) \propto G_1(1, 1) + G_1(2, 2) + 2\Re G_1(2, 1), \quad (91)$$

$$G_1(\mathbf{r}_2, t_2; \mathbf{r}_1, t_1) = \langle \hat{\mathcal{E}}^{(-)}(\mathbf{r}_2, t_2) \hat{\mathcal{E}}^{(+)}(\mathbf{r}_1, t_1) \rangle, \quad (92)$$

where $G_1(2, 1)$ is short for $G_1(\mathbf{r}_2, t_2; \mathbf{r}_1, t_1)$ etc. It is seen from Eq. (91) that the intensity on the second screen consists of three contributions: First two terms represent the intensities caused by each of the pinholes in the absence of the other, whereas the third term gives rise to interference effects.

For a symmetric configuration (equal slit width, homogeneous illumination, $G_1(1, 1) = G_1(2, 2)$) the visibility of the fringes is given by the magnitude of the normalized correlation function $g_1(1, 2)$

$$\mathcal{V} = \frac{I_{max} - I_{min}}{I_{max} + I_{min}} = |g(2, 1)|^2, \quad (93)$$

$$g_1(\mathbf{r}_2, t_2; \mathbf{r}_1, t_1) = \frac{G_1(\mathbf{r}_2, t_2; \mathbf{r}_1, t_1)}{\sqrt{G_1(1, 1)G_1(2, 2)}}. \quad (94)$$

Coherence (i.e. the possibility of interference) of light as measured with the double slit experiment is therefore a measure of correlation in the EMF.

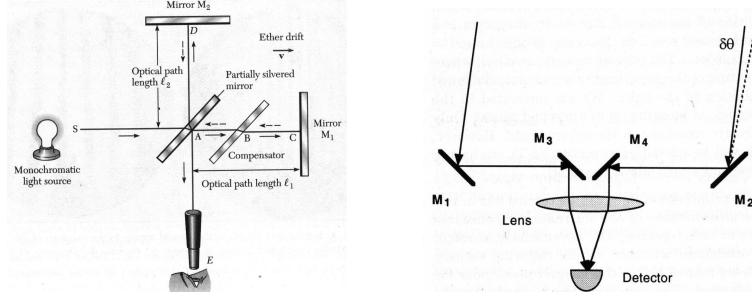


Figure 12. Sketch of the Michelson interferometer (left) and Michelson stellar interferometer (right). With these instruments the temporal and spatial correlation of the EMF can be measured independently. According to Bachor[38].

The Michelson interferometers – as depicted in Figs. 12 – are even better suited to investigate coherence properties as these instruments separately measure the temporal and spatial dependencies of $G_1(2, 1)$.

Prior to the invention of the laser, coherent light was made out of “chaotic” radiation by (wave length) filters and apertures. Here, the visibility in the Michelson interferometers vanishes (and remains zero!) if the distance between the arms becomes larger than the (longitudinal) coherence length $l_{coh} = ct_{coh}$ (point like source of spectral width $\Delta\lambda$) or larger than the (transversal) coherence diameter d_{coh} (monochromatic source of angular diameter $\Delta\theta$)

$$\text{Coherence time:} \quad t_{coh} = \frac{2\pi}{\Delta\omega} = \frac{\lambda_0^2}{c\Delta\lambda}$$

$$\text{Coherence diameter:} \quad d_{coh} = \frac{2\pi}{\Delta k} = 1.22 \frac{\lambda}{\Delta\theta}$$

The numerical factor of 1.22 holds for a circular light source. Note, the vanishing of the interference pattern is not the result of interference but of the shift of individual patterns which are produced independently by each frequency component or each volume element of an extended source[41].

The first star which was measured by Michelson and Pease with the 20ft (=6m armlength) stellar interferometer at Mt. Wilson observatory was the supergiant Betelgeuze in the stellar configuration of Orion ($\Delta\theta = 43 \times 10^{-3}$ seconds of an arc). Turbulence in the atmosphere severely affected these measurements and all efforts to increase the armlength proved to be unsuccessful. Hence, in total only 6 stars could be studied.

Examples:

$$\begin{array}{lll} \text{red Cd-line: } \lambda_0 = 643.8\text{nm}, & \Delta\lambda = 0.0013\text{nm}, & l_{coh} = 32\text{cm}. \\ \text{sun:} & \lambda_0 = 2.4\mu\text{m}, & \Delta\theta = 32', & d_{coh} = 316\text{m}. \end{array}$$

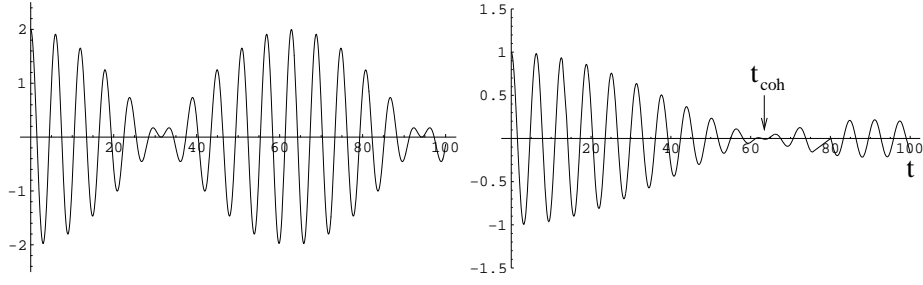


Figure 13. First order coherence functions as a function of time. (Left:) Two modes with $\omega_j = (1 \pm 0.05)\omega_0$ (left) and (right:) many uncorrelated modes with a “box” spectrum centered at ω_0 and full width $\Delta\omega = 0.1\omega_0$.

5.2.1. Examples for G_1

We study two examples for the (first order) classical coherence functions.

a) Single mode (deterministic/stochastic) field.

$$G_1(\mathbf{r}_2, t_2; \mathbf{r}_1, t_1) = \langle |a_{\mathbf{k},\sigma}|^2 \rangle \exp(-i[\mathbf{k}(\mathbf{r}_2 - \mathbf{r}_1) - \omega_{\mathbf{k}}(t_2 - t_1)]) \quad (95)$$

Obviously, this correlation function is (apart from the numerical value of $\langle |a_{\mathbf{k},\sigma}|^2 \rangle$) the same for a deterministic and a stochastic single mode field and displays maximum contrast.

b) Many statistically independent modes (of equal polarization) and intensity profile: $I(\omega_{\mathbf{k}}) = |\mathcal{E}(\omega)|^2$, $\langle \hat{a}_{\mathbf{k}',\sigma'}^* a_{\mathbf{k},\sigma} \rangle = I(\omega_{\mathbf{k}})\delta_{\mathbf{k},\mathbf{k}'}\delta_{\sigma,\sigma'}$.

$$\mathcal{E}^{(+)}(\mathbf{r}, t) = \sum_{\mathbf{k}} a_{\mathbf{k},\sigma} e^{i(\mathbf{k}\mathbf{r} - \omega_{\mathbf{k}}t)}, \quad (96)$$

$$G_1(\mathbf{r}_2, t_2; \mathbf{r}_1, t_1) = \sum_{\mathbf{k}} I(\omega_{\mathbf{k}}) e^{-i[\mathbf{k}(\mathbf{r}_2 - \mathbf{r}_1) - \omega_{\mathbf{k}}(t_2 - t_1)]}. \quad (97)$$

In particular, we have at the same space point, $\mathbf{r}_2 = \mathbf{r}_1 = \mathbf{r}$, (as measured by a Michelson interferometer)

$$G_1(t_2 - t_1) = G_1(\mathbf{r}, t_2; \mathbf{r}, t_1) = \int_0^\infty I(\omega) e^{i\omega(t_2 - t_1)} \frac{d\omega}{2\pi} \quad (98)$$

For a Gaussian line centered at $\omega_0 > 0$

$$I(\omega) = I_0 e^{-\frac{(\omega - \omega_0)^2}{2(\Delta\omega)^2}}, \quad (99)$$

$$G_1(t) = \sqrt{2}I_0\Delta\omega e^{-\frac{(\Delta\omega t)^2}{2}} e^{i\omega_0 t}. \quad (100)$$

Some examples are depicted in Figs. 11 and 13.

Concerning their coherence properties, the filtered many mode field is virtually indistinguishable from the single mode field provided $t < t_{coh}$.

(This follows also from the Wiener–Khinchine theorem.) The same reasoning holds for filtering within various directions in \mathbf{k} -space by apertures (spatial coherence).

NB: A convenient model to describe wide-band stochastic processes is “white noise”, $I(\omega) = \text{const.}$ This leads to completely uncorrelated fields with no interference fringes.

Problem:

P6: Study the case of two statistically independent modes of equal intensity and discuss the interference pattern for the Na-D doublet $\lambda_0 = 589\text{nm}$, $\Delta\lambda = 0.6\text{nm}$ (Fizeau 1862).

5.3. INTENSITY CORRELATIONS: HANBURY–BROWN & TWISS EFFECT

In the previous section we considered first order field correlation. For fields with identical spectral properties the classical and quantum treatments leads to the same result. This can be different when studying intensity (=photon) correlations.

A bit of history: The intrinsic problems of the Michelson stellar interferometer – mechanical instability at armlength longer than 6m, and the effect of atmospheric turbulence, were overcome by the invention of the *intensity interferometer*. The idea dates back to 1949 where R. Hanbury Brown, a radio astronomer at Jodrell Bank, was trying to design a radio interferometer which would solve the intriguing problem of measuring the angular size of the most prominent radio sources: Cygnus A and Cassiopeia A. If, as some people thought at that time their angular size is as small as the largest visible stars, then global base lines would be needed and a coherent superposition of the signals would be impossible in praxis (around 1950!).

The new and unconventional idea was to correlate (low frequency) intensities instead of superimposing (high frequency) amplitudes. First, a pilot model was built in 1950 and was tested by measuring the angular diameter of the sun at 2.4m wavelength, and, subsequently, the radio sources Cygnus A and Cassiopeia A. The intermediate-frequency outputs of the completely independent superheterodyne receivers were rectified in square law detectors and bandpass filtered (1...2.5KHz). Then, the LF outputs were brought together by radio links (or telephone!). After analogue multiplication of the LF signals and integration, the correlator output

$$G_2^{cl}(\mathbf{r}_2, t_2; \mathbf{r}_1, t_1) = \langle I(\mathbf{r}_2, t_2) I(\mathbf{r}_1, t_1) \rangle, \quad (101)$$

displayed the expected correlations, see Fig. 14. (A constant term has been subtracted by LF bandpass filtering so that $G_2(2,1) \rightarrow 0$ for large

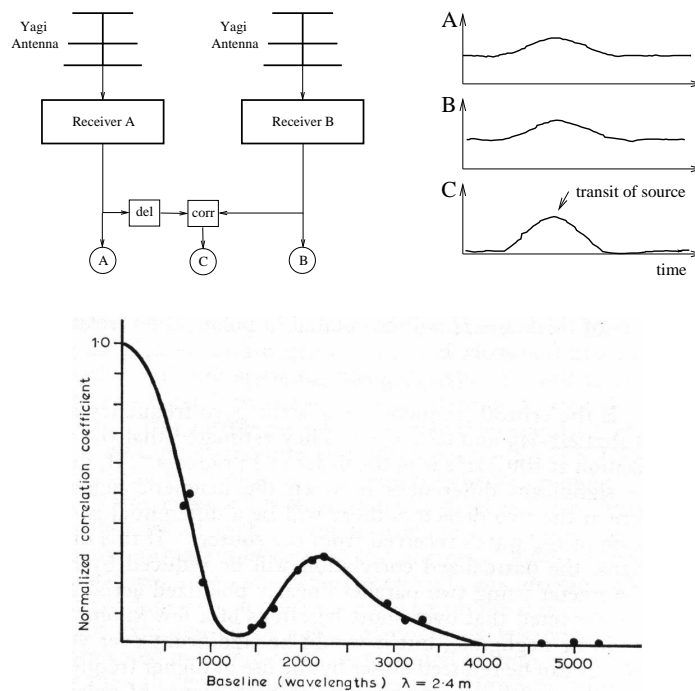


Figure 14. (a) Sketch of the RF interferometer at $\lambda = 2.4\text{m}$ wavelength. (b) Output of the individual receivers A,B and correlation C showing the transit of a radio source through the arial beam. (c) Normalized correlation function for the radio source Cygnus A which consists of two almost equal components with an angular diameter of $45''$ and a separation of $1'25''$. According to Hanbury Brown[42].

separation of \mathbf{r}_2 and \mathbf{r}_1)). However, to the great disappointment of the investigators, the adventure was over at a separation of less than 5km. This experiment could have been done by conventional technique!

For many independent modes, Eq. (101) can be evaluated in the same way as for G_1 ,

$$G_2^{cl}(\mathbf{r}_2, t_2; \mathbf{r}_1, t_1) = \sum_{\mathbf{k}} \left(\langle |a_{\mathbf{k}}|^4 \rangle - 2\langle |a_{\mathbf{k}}|^2 \rangle^2 \right) + |G_1(0, 0; 0, 0)|^2 + |G_1(\mathbf{r}_2, t_2; \mathbf{r}_1, t_1)|^2. \quad (102)$$

Moreover, for Gaussian thermal light $\langle |a_{\mathbf{k}}|^4 \rangle = 2\langle |a_{\mathbf{k}}|^2 \rangle^2$, so that the first term of Eq. (102) drops out. In all other cases this contribution is negative so that the “contrast” in $G_2(2, 1)$ for adjacent (\mathbf{r}_2, t_2) , (\mathbf{r}_1, t_1) and distant arguments is smaller than for thermal radiation. For thermal radiation, intensity correlation measurements yield the same information as conventional first order coherence experiments, e.g. using the Michelson interferometers.

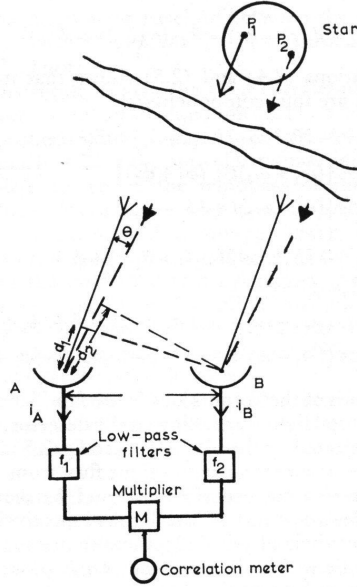


Figure 15. Optical intensity interferometer proposed and developed by Hanbury Brown and Twiss to measure the angular diameter of stars. According to Hanbury Brown[42].

The optical analogue of the intensity interferometer seemed to be straightforward: Antennas and receivers will respectively be replaced by mirrors and photodetectors, as sketched in Fig. 15. In principle, the theory is the same for all wavelengths but the trouble of course was worrying about photons. In the RF spectrum the energy flows rather smoothly whereas in the optical region energy comes in “photon–bursts”, see Fig. 3. A correlator (or coincidence counter) measures the combined absorption of photons at different space time points (\mathbf{r}_2, t_2) and (\mathbf{r}_1, t_1) . As a result, we have

$$G_2(\mathbf{r}_2, t_2; \mathbf{r}_1, t_1) = \langle \hat{\mathcal{E}}^{(-)}(\mathbf{r}_2, t_2) \hat{\mathcal{E}}^{(-)}(\mathbf{r}_1, t_1) \hat{\mathcal{E}}^{(+)}(\mathbf{r}_2, t_2) \hat{\mathcal{E}}^{(+)}(\mathbf{r}_1, t_1) \rangle. \quad (103)$$

Note, the sequence of operators matters, creation and destruction operators are in “normal order” (creation operators left to the destruction operators). Nevertheless, for thermal radiation, the classical result given by Eq. (102) remains valid.

If one thinks in terms of photons one must accept that thermal photons at two well separated detectors are correlated – they tend to “arrive” in pairs (“photon bunching”)! But how, if the photons are emitted at random in a thermal source, can they appear in pairs at two well separated detectors? What about the sacred number–phase uncertainty relation?

$$\Delta \hat{N} \Delta \hat{\Phi} \geq 1. \quad (104)$$

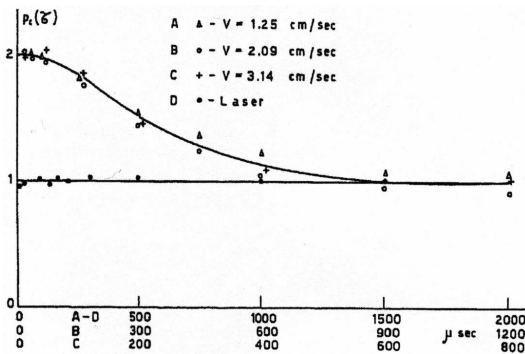


Figure 16. Photon coincidences for single mode chaotic light and laser light. Coherence time of the chaotic light depends on the speed v of the rotating ground glass disk. According to Arecchi et al.[20].

Wouldn't a photon number measurement destroy phase relations and, hence, all interference phenomena? However, for an (intensity) interferometer the absolute phase is not relevant, only the phase difference matters and this difference is not touched by Eq. (104).

Eventually, this problem was settled by experiment which clearly shows that photon bunching exists in thermal radiation [23, 24]. Later on, a well functioning stellar interferometer was built in Australia. More on the exciting scientific story about this instrument and its history can be found in Hanbury Brown's book[42].

Today, the photon bunching effect can be simply demonstrated with an artificial "chaotic" source which synthesizes pseudothermal light by passing laser radiation through a rotating ground glass disk with long adjustable coherence times ("Martienssen lamp")[25], see Fig. 16.

It is instructive to define a coincidence ratio

$$R = \frac{C - C_{rand}}{C_{rand}} = \frac{(\Delta n)^2 - \langle n \rangle}{(\langle n \rangle)^2}, \quad (105)$$

where $C \propto G_2(1, 1) = \langle \hat{N}(\hat{N} - 1) \rangle$. The number of random coincidences is proportional to $C_{rand} = G_2(2, 1) = \langle \hat{N} \rangle^2$ when the separation of $\mathbf{r}_2, t_2, \mathbf{r}_1, t_1$ is much larger than the coherence area/time.

$$\begin{array}{lll} \text{Coherent states:} & (\Delta N)^2 = \bar{n} & R = 0, \\ \text{thermal states:} & (\Delta N)^2 = \bar{n}(\bar{n} + 1) & R = 1, \\ \text{number states:} & (\Delta N)^2 = 0 & R = -\frac{1}{\bar{n}}. \end{array}$$

Classical states have photon number distributions which are always broader than a Poissonian, i.e., $(\Delta N)^2 \geq \bar{n}$, hence, the correlation ratio is positive: Classical states always show "photon bunching". The α states as generated

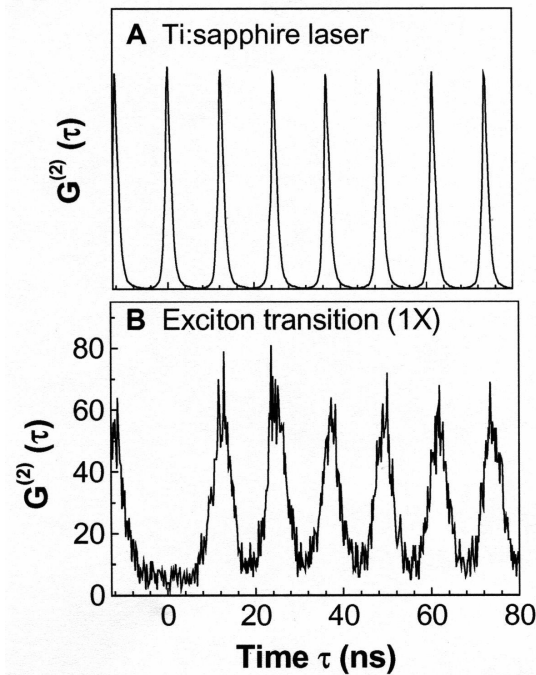


Figure 17. Single photon turnstile device. (A) Unnormalized second order correlation function of a mode locked Ti:sapphire laser (FWHM=250 fs) and (B) a single quantum dot excitonic ground state (1X) emission under pulsed excitation conditions (82MHz). According to Michler et al.[30].

by an amplitude stabilized laser, represent the optimum classical state with respect to photon fluctuations.

On the other hand, states which have less photon number fluctuations than a Poissonian, e.g., the number states, show “antibunching”, i.e., the photons prefer to “come” not too close, see Fig. 22. In particular, the single photon state $|n = 1\rangle$ is the most nonclassical state one can think of! Obviously, photon bunching is not a “typical Bose property”.

The generation of nonclassical light (which still showed “photon bunching”) was first demonstrated in 1977 by Kimble, Dagenais, and Mandel[27]; the first clear evidence for antibunching, $R \approx 0$, was presented by Diedrich and Walther[28] in 1987, using a single Mg-Ion in a Paul-trap.

For a review about photon antibunching, see the article by Paul[29]. Presently, nonclassical photon states became attractive in semiconductor optics in connection with quantum communication. For instance Michler et al.[30] have developed a “Quantum dot single photon turnstile device”, see Fig. 17.

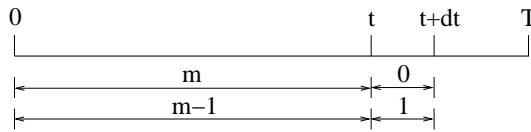


Figure 18. Time intervals used for the derivation of $P_m(T)$.

5.4. PHOTON COUNTING

The number of photons which a counter records in any interval of time fluctuates randomly. In a simple counting experiment we may imagine that the counter is exposed to the radiation field for a fixed time interval T . After a time delay T_{del} , which is long compared to the coherence time of the light, the original experiment is repeated, and a second number of counted photons is recorded and so on. The results can be expressed by a probability distribution $P_m(T)$ for the counting of m photons during an observation time T .

We consider a particular period of counting $[t, t+T]$ as shown in Fig. 18. There are two ways in which m photons can be counted in the periods between times t and $t+dt$. The probability that more than one photon being counted during the time interval dt is proportional to $(dt)^2$ and, thus, negligible.

$$P_m(t+dt) = P_m(t) [1 - p(t) dt] + P_{m-1}(t) p(t) dt \quad (106)$$

Rearranging terms and using $P_m(t+dt) - P_m(t) = \dot{P}_m(t)dt + O(dt)^2$ we obtain a chain of coupled differential equations

$$\frac{dP_m(t)}{dt} = \zeta I(t) [P_{m-1}(t) - P_m(t)], \quad (107)$$

$$P_{-1} = 0, \quad P_0(0) = 1, \quad P_m(0) = 0 \quad (m > 1), \quad (108)$$

which can be solved by recursion.

The probability that no photon to be recorded during time t becomes

$$P_0'(t) = -\zeta I(t) P_0(t), \quad (109)$$

$$P_0(T) = e^{-\zeta \bar{I}(T)T}, \quad (110)$$

$$\bar{I}(T) = \frac{1}{T} \int_0^T I(t') dt'. \quad (111)$$

$\bar{I}(T)$ is the mean intensity during the observation time T . The remaining counting functions $P_m(T)$ can be obtained from Eq. (107), beginning with $m = 1$ and proceeding to higher values. As a result, we obtain

$$P_m(T) = \frac{[\zeta \bar{I}(T)T]^m}{m!} e^{-\zeta \bar{I}(T)T}. \quad (112)$$

Equation (112) gives the count distribution obtained in a series of measurements all beginning at the same time ($t = 0$), where the same time duration T , and the same $I(t)$ is implied. This is impossible in practice: Counting periods run consecutively rather than simultaneously. Photon measurements imply the absorption of photons so that a single photon can be counted only once! The intensity $\bar{I}(T)$ in general fluctuates for different members of the ensemble and the measured photon count distribution is an average of $P_m(T)$ over a large number of different starting times (which are separated in time by a period much larger than the coherence time).

$$\bar{P}_m(T) = \langle P_m(T) \rangle. \quad (113)$$

A nice introduction to photon counting is still Loudon's book[34].

5.4.1. Examples

a) Constant intensity (amplitude stabilized single mode laser).

$I(t) = I_0$ is constant so that the quantity to be averaged is time-independent.

$$\bar{P}_m(T) = \exp(-\bar{m}) \frac{\bar{m}^m}{m!}, \quad \bar{m} = \zeta I_0 T. \quad (114)$$

This is a *Poissonian distribution* with a mean photon count number \bar{m} , see Fig. 19. This distribution has been already discussed in Section 4.4.3.

The fluctuations which occur for a beam of constant intensity are called *particle fluctuations*. They are due to the discrete nature of the photoelectric process in which energy can be removed from the light beam only in whole quanta $\hbar\omega$.

b) Chaotic (thermal) light, long time limit ($T \gg t_{coh}$).

Another important case for which the Poisson-distribution Eq. (114) holds, follows from the fact that $\bar{I}(T)$ can be constant even if $I(t)$ is a fluctuating quantity. This case holds for chaotic light (of arbitrary type) if the time of measurement is much larger than the coherence time of the light, so that all fluctuations are averaged out during a long time period.

c) Chaotic (thermal) light, short time limit ($T \ll t_{coh}$).

The probability distribution for the instantaneous intensity of thermal light is given by Eq. (29). With the usual ergodic hypothesis the time average in Eq. (113) is converted to an ensemble average over the distribution $p(I) = \exp(-I/I_{av})/(\pi I_{av})$, Eq. (29), leading to

$$\bar{P}_m(T) = \int_0^\infty p(I) P_m(T) dI = \frac{\bar{m}^m}{[\bar{m} + 1]^{m+1}} = b_m. \quad (115)$$

b_m is the Bose-Einstein distribution function, see Fig. 20, which we have already met in Section 4.4.5.

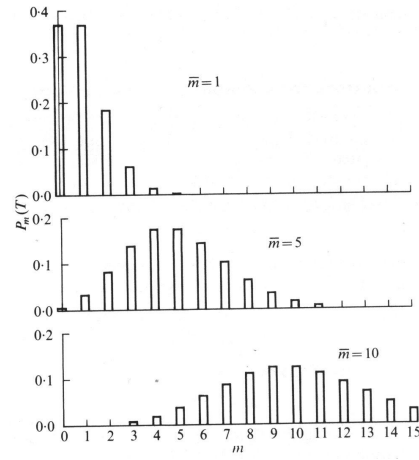


Figure 19. Poisson form of the photon count distribution for light beams of constant intensity (Single mode laser well above threshold). According to Loudon[34].

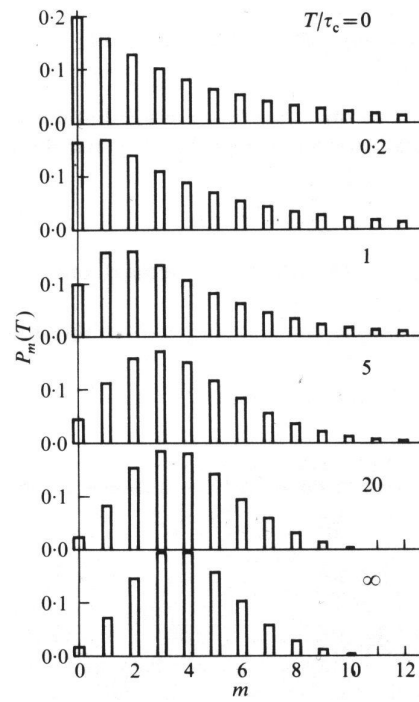


Figure 20. Photon count distribution for chaotic (thermal) single mode light for $\bar{m} = 4$ and different counting times T . According to Loudon[34].

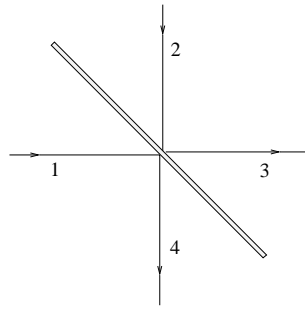


Figure 21. Sketch of a beam splitter. Modes 1 and 2 are transformed into 3, 4.

The photon count distributions derived above are based on a semiclassical approach where the intensity $\bar{I}(T)$ is treated as a classical quantity. The quantum mechanical formulation (in the Heisenberg picture) has to take into account that the operators $\hat{\mathcal{E}}^{(-)}(\mathbf{r}, t)$, $\hat{\mathcal{E}}^{(+)}(\mathbf{r}, t)$ do not commute. Formally, the result is similar to Eq. (112), but the evaluation is much more laborious than in the semiclassical case. For coherent and thermal states the count distributions have the same form, however, this is not true in general. For details we refer to the book by Klauder and Sudarshan[37].

5.5. BEAM SPLITTERS

Optical components like lenses, mirrors, polarizers etc., are used in quantum optics to transform one mode in another. For example, let us consider a beam splitter which transforms an incoming wave beam with field \mathcal{E}_1 into a transmitted and a reflected beam with fields $\mathcal{E}_3, \mathcal{E}_4$, respectively. However, there is also a second possible input axis defined, such that \mathcal{E}_2 would produce the output waves in the same place and propagating in the same direction as \mathcal{E}_3 and \mathcal{E}_4 (e.g. as used in a Mach-Zehnder interferometer). The complex amplitudes of the EMF transform according to

$$\begin{pmatrix} a_3 \\ a_4 \end{pmatrix} = \begin{pmatrix} \sqrt{1-R} & \sqrt{R} \\ -\sqrt{R} & \sqrt{1-R} \end{pmatrix} \begin{pmatrix} a_1 \\ a_2 \end{pmatrix}. \quad (116)$$

R is the (intensity) reflection coefficient. (Note, there is a phase jump of π of the reflected beams). In a quantum treatment the complex amplitudes will be replaced by destruction operators. In quantum optics, the case of “no incident wave” refers to the vacuum state of that mode rather than to “zero field”.

In quantum optics amplitudes a_j become operators \hat{a}_j and Eq. (116) represents a unitary basis transformation. A beam splitter does not “split” photons, rather it acts as a random selector which divides the incident flow of photons in a reflected and a transmitted one. As a consequence, the

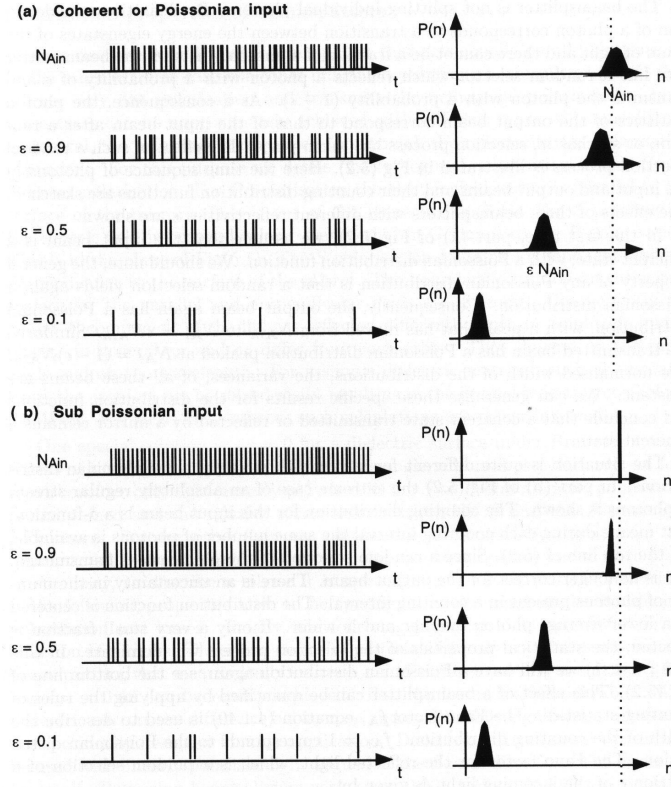


Figure 22. Change of photon statistics of an n photon state after passing a beam splitter. (a) Coherent state, (b) n -photon state. According to Bachor[38].

photon statistics of the reflected/transmitted beams correspond to that of the input beam after a random selection process has taken place. For a coherent state with a Poissonian distribution, a random selection yields again a Poissonian, hence a coherent state remains a coherent state after reflection or transmission through a mirror, yet with a reduced value of α .

The situation may be different for states with a non-Poissonian photon distribution. For an incident $|n\rangle$ -photon state the probability that $k(\leq n)$ photons are reflected ($n - k$ being transmitted) becomes

$$p_k^{(n)} = \binom{n}{k} R^k (1 - R)^{n-k}, \quad k = 0, 1, \dots, n. \quad (117)$$

The binominal coefficient arises from the indistinguishability of the photons. Hence, an incident photon state with distribution p_n transforms according

to

$$p_k^{ref} = \sum_n p_n \binom{n}{k} R^k (1-R)^{n-k}, \quad (118)$$

$$p_k^{tr} = \sum_n p_n \binom{n}{k} (1-R)^k R^{n-k}. \quad (119)$$

In addition to coherent states, thermal states likewise have the remarkable property that the photon statistics remains unchanged when passing the splitter (yet with a reduced mean photon number $\bar{k} = (1-R)\bar{n}$, see Fig. 22). For details see, e.g., Paul[32] or Bachor[38].

6. Outlook

Die ganzen Jahre bewusster Grübeleien haben mich der Antwort der Frage “Was sind Lichtquanten” nicht näher gebracht. Heute glaubt zwar jeder Lump, er wisse es, aber er täuscht sich. . .

Literal translation:

All the years of willful pondering have not brought me any closer to the answer to the question “what are light quanta”. Today every good-for-nothing believes he should know it, but he is mistaken. . .

ALBERT EINSTEIN²

But, in contrast to Einstein, most of us have given up any hope for objective realism. . .

For a discussion on conceptual difficulties and different interpretations of Quantum Mechanics see Costa’s interdisciplinary article in this book.

7. Acknowledgement

Thanks to Prof. Di Bartolo and his team, the staff of the Majorana Center, and all the participants which again provided a wonderful time in a stimulating atmosphere.

² In a letter to M. Besso, 1951. See first page of Ref.[32].

References

1. M. Planck, Verh. Dtsche. Phys. Ges. **2**, 202, 237 (1900), *Theorie der Wärmestrahlung*, 6. Auflage, J. A. Barth, Leipzig (1966).
2. P. Lenard, *Ueber die lichtelektrische Wirkung*, Annalen der Physik, **8**, 149–198 (1902).
3. A. Einstein, *Über einen die Erzeugung und Verwandlung des Lichts betreffenden heuristischen Gesichtspunkt*, Annalen der Physik, **17**, 132 (1905).
4. G. Breit, *Are Quanta Unidirectional?*, Phys. Rev. **22**, 314 (1923).
5. A. H. Compton, *The Spectrum of Scattered X-Rays*, Phys. Rev **22**, 409 (1923).
6. G. I. Taylor, Proc. Cambridge Phil. Soc. **15**, 114 (1909).
7. A. J. Dempster and H. F. Batho, *Light Quanta and Interference*, Phys. Rev. **30**, 644 (1927).
8. E. O. Lawrence and J. W. Beams, *The element of time in the photoelectric effect*, Phys. Rev. **32**, 478 (1928).
9. L. Janossy, *Experiments and Theoretical Considerations Concerning The Dual Nature of Light*, in H. Haken and M. Wagner (eds.), Cooperative Phenomena, Springer Verlag, Berlin (1973).
10. A. T. Forrester, R. A. Gudmundsen, and P. O. Johnson, *Photoelectric Mixing of Incoherent Light*, Phys. Rev. **99**, 1691 (1955).
11. P. Grangier, G. Roger, and A. Aspect, *Experimental Evidence for Photon Anticorrelation Effects on a Beam Splitter: A New Light on Single-Photon Interferences*. Eur. Phys. Lett. **1**, 173 (1986). See also Physics World, Feb. (2003).
12. P. A. M. Dirac, *The Quantum Theory of the Emission and Absorption of Radiation*, Proc. Roy. Soc. A **114**, 243 (1927), see also *The Principles of Quantum Mechanics*, fourth edition, Oxford, At the Clarendon Press (1958).
13. E. Schrödinger, *Die Naturwissenschaften*, **28**, 664 (1926), reprinted in: *Collected Papers on Wave Mechanics by E. Schrödinger*, Chelsea, New York (1982).
14. J. C. Mather et al., *A preliminary Measurement of the Cosmic Microwave Background Radiation by the Cosmic Background Explorer (COBE) Satellite*, The Astrophysical Journal, **354**, L37-L40, (1990).
15. R. J. Glauber, *The Quantum Theory of Optical Coherence*, Phys. Rev. **130**, 2529 (1963), *Coherent and Incoherent States of the Radiation Field*, Phys. Rev. **131**, 2766 (1964), and in Ref.[45, 46].
16. S. F. Jacobs, *How Monochromatic is Laser Light*, Am. J. Phys. **47**, 597 (1979).
17. D. Stoler, *Equivalence Class of Minimum Uncertainty Packets*, Phys. Rev. D**1**, 3217 (1970).
18. H. P. Yuen, *Two-photon coherent states of the radiation field*, Phys. Rev. A**13**, 2226 (1976).
19. C. M. Caves, *Quantum-mechanical noise in an interferometer*, Phys. Rev. D**23**, 1693 (1981).
20. F. T. Arecchi, E. Gatti, and A. Sona, *Time distribution of Photons From Coherent and Gaussian Sources*, Phys. Lett. **20**, 27 (1966).
21. D. F. Walls, *Squeezed states of light*, Nature **306**, 141 (1983).
22. E. Giacobino, C. Fabre, and G. Leuchs, Physics World **2**, Feb., p.31 (1989).
23. R. Hanbury Brown and R. Q. Twiss, *Correlations . . .*, Nature **177**, 27 (1956).
24. G. A. Rebka and R. V. Pound, *Time-Correlated Photons*, Nature **180**, 1035 (1957).
25. W. Martienssen and E. Spiller, *Coherence and Fluctuations in Light Beams*, Am. J. Phys. **32**, 919 (1964).

26. H. J. Kimble, M. Dagenais, and L. Mandel, *Photon Antibunching in Resonance Fluorescence*, Phys. Rev. Lett **39**, 691 (1977).
27. M. Dagenais and L. Mandel, *Investigations of two-time correlations in photon emissions from a single atom*, Phys. Rev. **A18**, 2217 (1978).
28. F. Diedrich and H. Walther, *Nonclassical Radiation of a Single Stored Ion*, Phys. Rev. Lett. **58**, 203 (1987).
29. H. Paul, *Photon Antibunching*, Rev. Mod. Phys. **54**, 1061 (1982).
30. P. Michler et al., *A Quantum Dot Single-Photon Turnstile Device*, Science **290**, 2282 (2000).
31. S. Strauf, P. Michler, M. Kluder, D. Hommel, G. Bacher, and A. Forchel, Phys. Rev. Lett. **89**, 177403-1 (2002).
32. H. Paul, *Photonen. Eine Einführung in die Quantenoptik*, B. G. Teubner Stuttgart, Leipzig (1999).
33. H. Haken, *Light*, Vols. I and II, North Holland (1981).
34. R. Loudon, *The Quantum Theory of Light*, Clarendon Press, Oxford (1973).
35. M. O. Scully and S. S. Zubairy, *Quantum Optics*, Cambridge University Press (1999).
36. W. H. Louisell, *Quantum Statistical Properties of Radiation*, Wiley (1973).
37. Klauder and E. G. C Sudarshan, *Quantum Optics*, W. A. Benjamin (1968).
38. H. A. Bachor, *A Guide to Experiments in Quantum Optics*, Wiley-VCH (1998).
39. E. G. Harris, *A Pedestrian Approach to Quantum Field Theory*, Wiley (1972).
40. L. D. Landau and E. M. Lifshitz, Vol. IVA, *Relativistische Quantenfeldtheorie*, Akademie Verlag, Berlin (1970).
41. M. Born and E. Wolf, *Principles of Optics*, Pergamon Press, 2nd ed., Oxford (1964).
42. R. Hanbury Brown, *The Intensity Interferometer*, Taylor and Francis (1974).
43. K.-H. Patke, D. Oberhauser, V. G. Lyssenko, J. M. Hvam, and G. Weimann, *Coherent generation and interference of excitons and biexcitons in GaAs/Al_xGa_{1-x}As quantum wells*, Phys. Rev. B **45**, 2413 (1993).
44. K. Razi Naqvi and S. Waldenström, *Revival, Mirror Revival and Collapse may occur even in a harmonic Oscillator Wavepacket*, Physica Scripta **62**, 12 (2000).
45. C. de Witt, A. Blandin, and C. Cohen-Tannoudji (eds), *Quantum Optics and Quantum Electronics*, Gordon and Breach (1965).
46. R. J. Glauber (ed.), *Quantum Optics*, Academic Press, New York (1969).
47. L. Mandel and E. Wolf, (eds.), *Coherence and Quantum Optics*, Plenum (1973).
48. N. Kroll, *Quantum Theory of Radiation*, in Ref.[45].
49. R.v.Baltz and C.F. Klingshirm, *Quasiparticles and Quasimomentum*, in: *Ultrafast Dynamics of Quantum Systems: Physical Processes and Spectroscopic Techniques*, NATO ASI series B Physics: Vol 372, edited by B. Di Bartolo, Plenum (1999).
50. J. F. Clauser *Localization of Photons*, in Ref.[47].
51. F. T. Arecchi, *Photocount distributions and field statistics*, in Ref.[46].

Solutions of the Problems

- P1: Time dependent Schrödinger equation: $\dot{x}_c = p_c$, $\dot{p}_c = -\omega_0^2 x_c + f(t)$.
- P2: $w(t) = [1 - \kappa \exp(-2it)] / [1 + \kappa \exp(-2it)]$, $u(t)$ from normalization.
 $v(t) = \nu / [\exp(it) + \kappa \exp(-it)]$, κ, ν are constants.
- P3: Use $\hat{b} = \mu \hat{a} + \nu \hat{a}^\dagger$, Eq. (43), and $\cosh^2 x - \sinh^2 x = 1$.
- P4: Energies can be non-equidistant but must be multiples of a unit.
- P5: Yes! Eq. (47) is a displaced oscillator. $\langle \hat{N} \rangle = \sum_{\mathbf{k}, \sigma} |j_{\mathbf{k}, \sigma}|^2 / (2\epsilon_0 \hbar \omega_{\mathbf{k}}^3)$.
- P6: See Born and Wolf[41], p. 320.